

**PIERRE  
AUGER**  
OBSERVATORY

# Experimental Constraints to high energy hadronic interaction models using the Pierre Auger Observatory part-I

(cosmic rays, the Auger detectors, event reconstruction, observations)

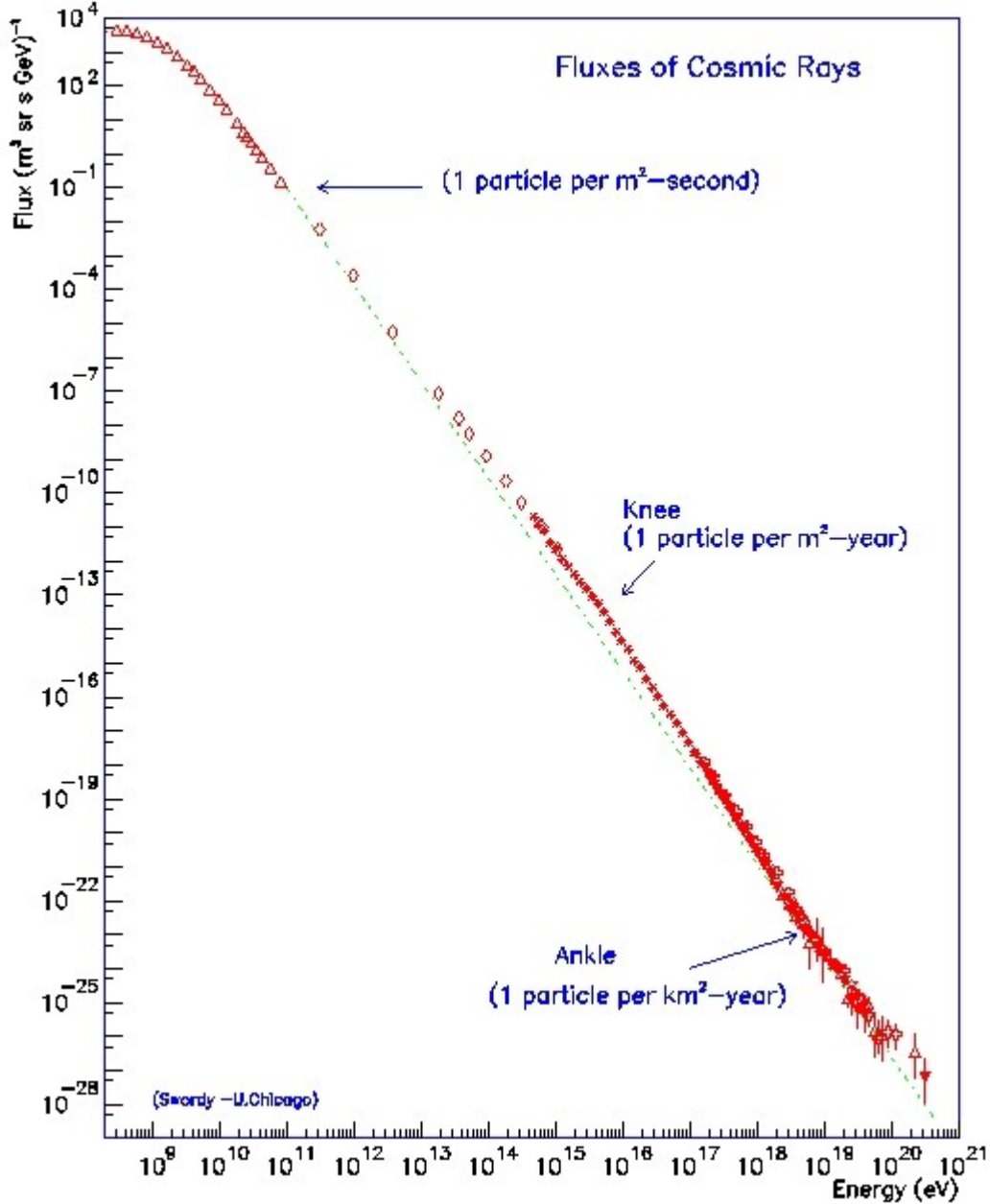
**Jose Bellido**



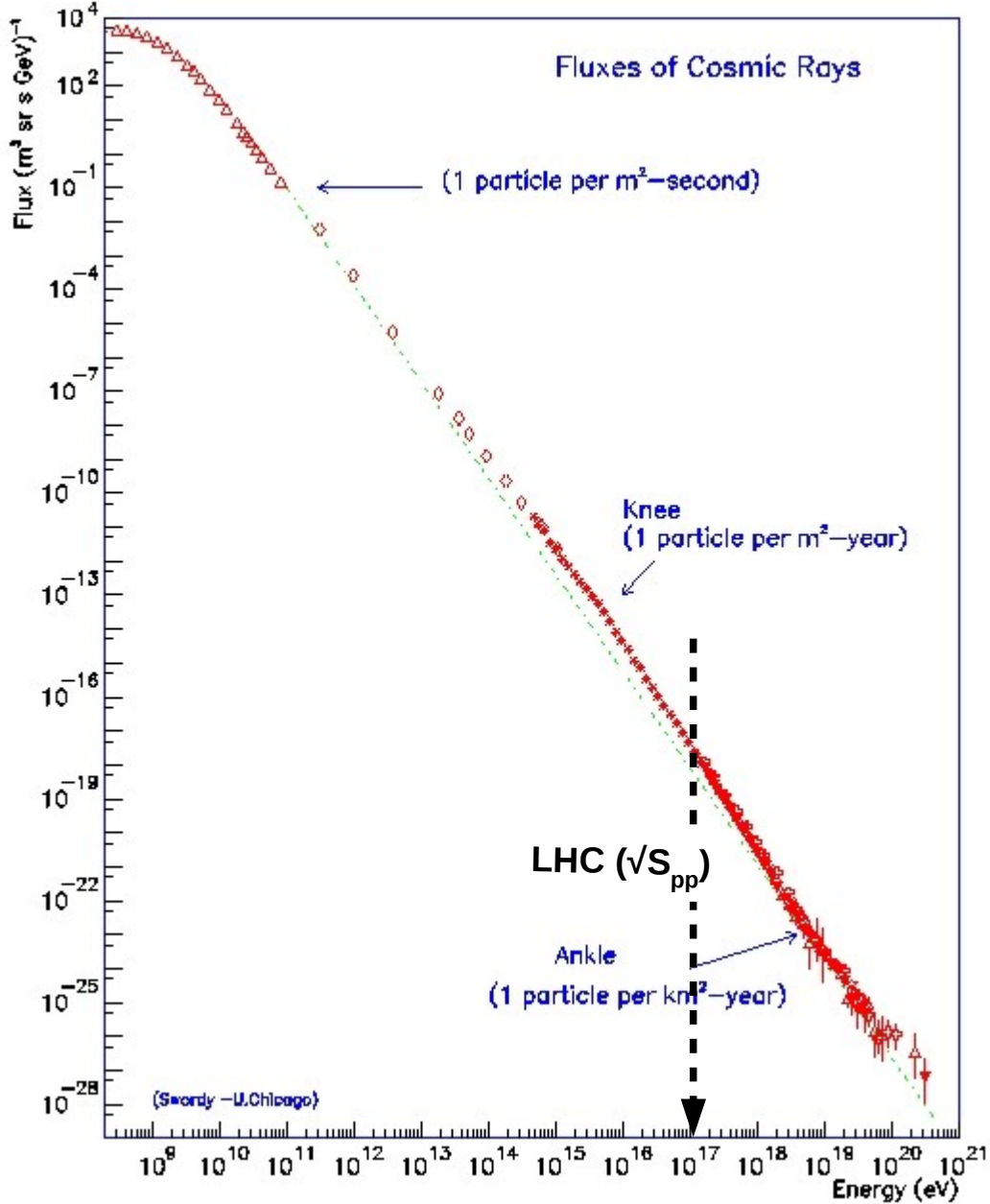
THE UNIVERSITY  
*of* ADELAIDE

QCD @ Cosmic Energies, 16 – 20 of May, 2016, Chalkida, Greece

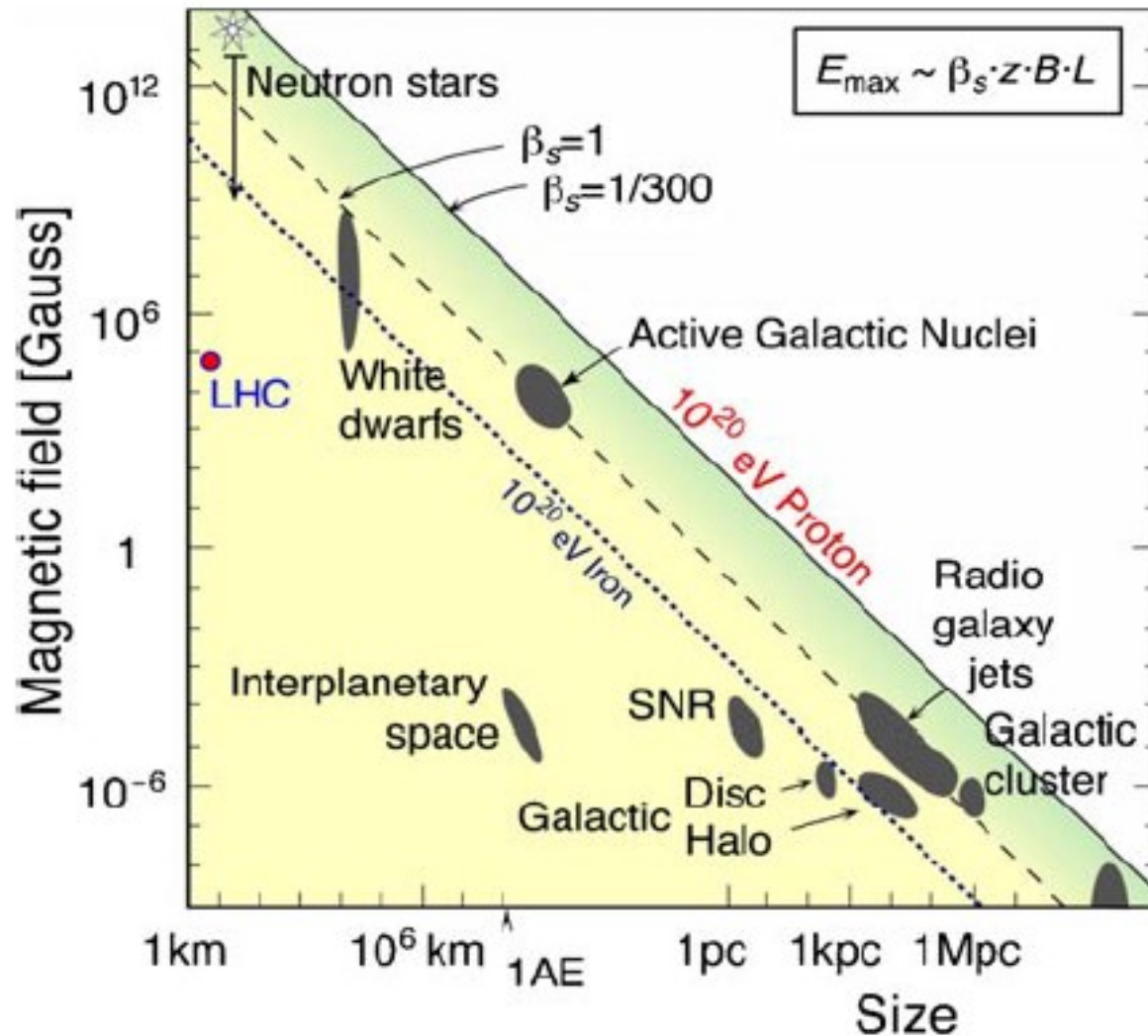
# Cosmic Rays flux as a function of energy



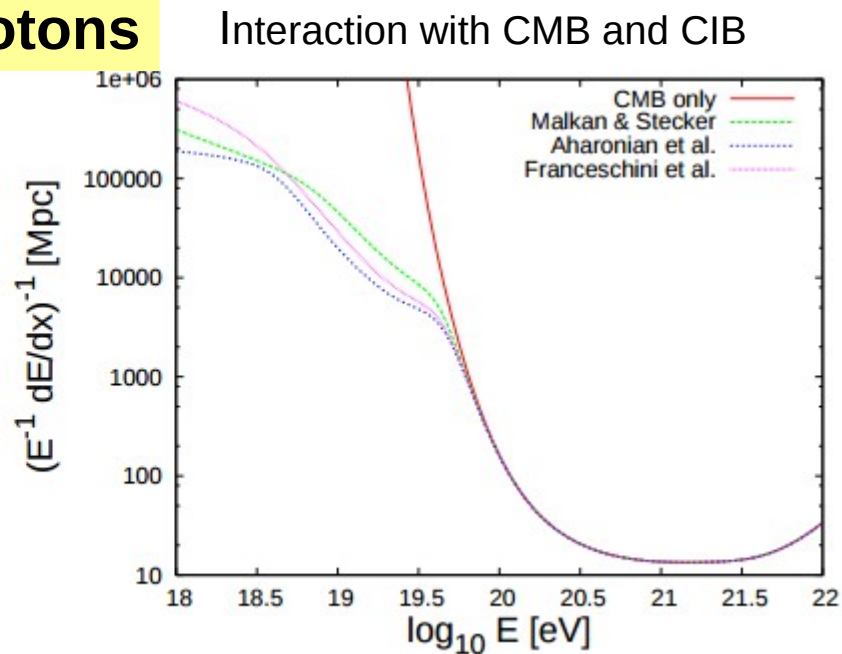
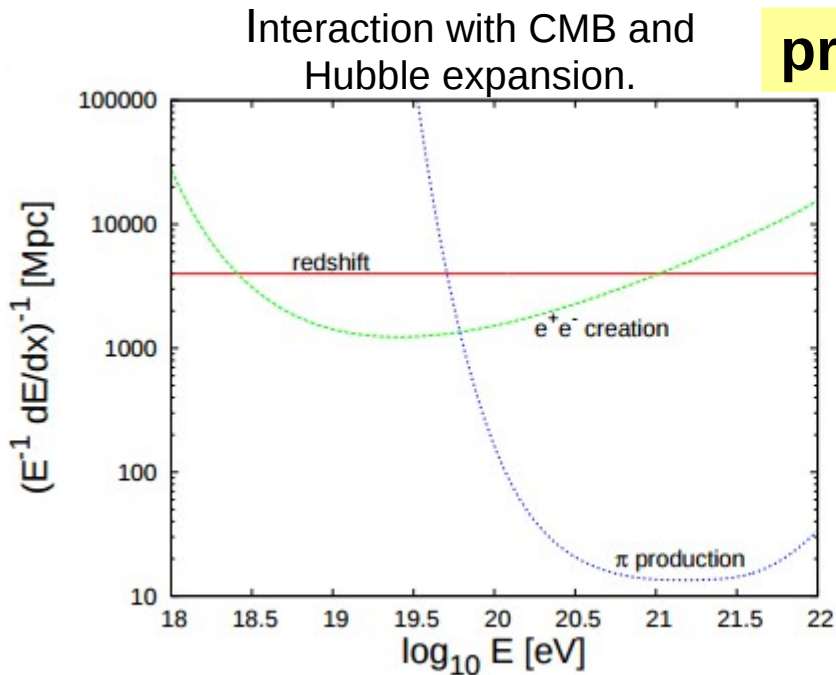
# Cosmic Rays flux as a function of energy



There is not clear explanation for cosmic rays with energies above  $10^{20}$  eV

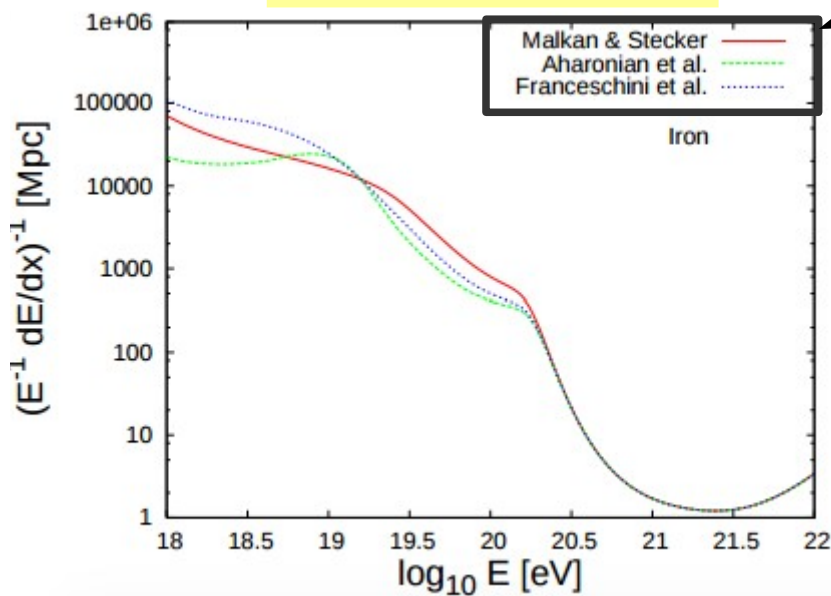


# Energy loss lengths for UHE cosmic rays propagating through the universe



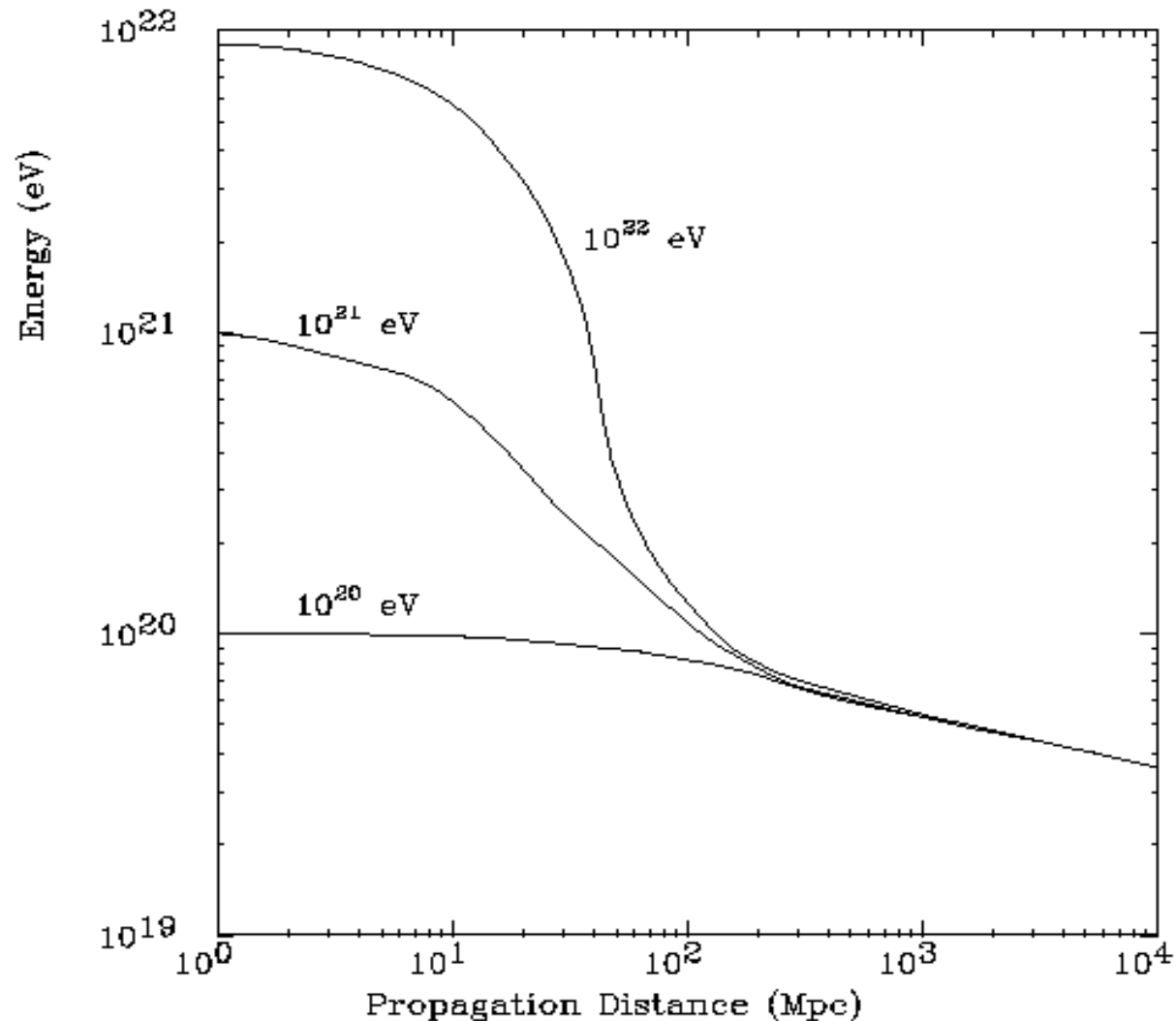
## Iron (photodesintegration)

Cosmic infrared background models (CIB)

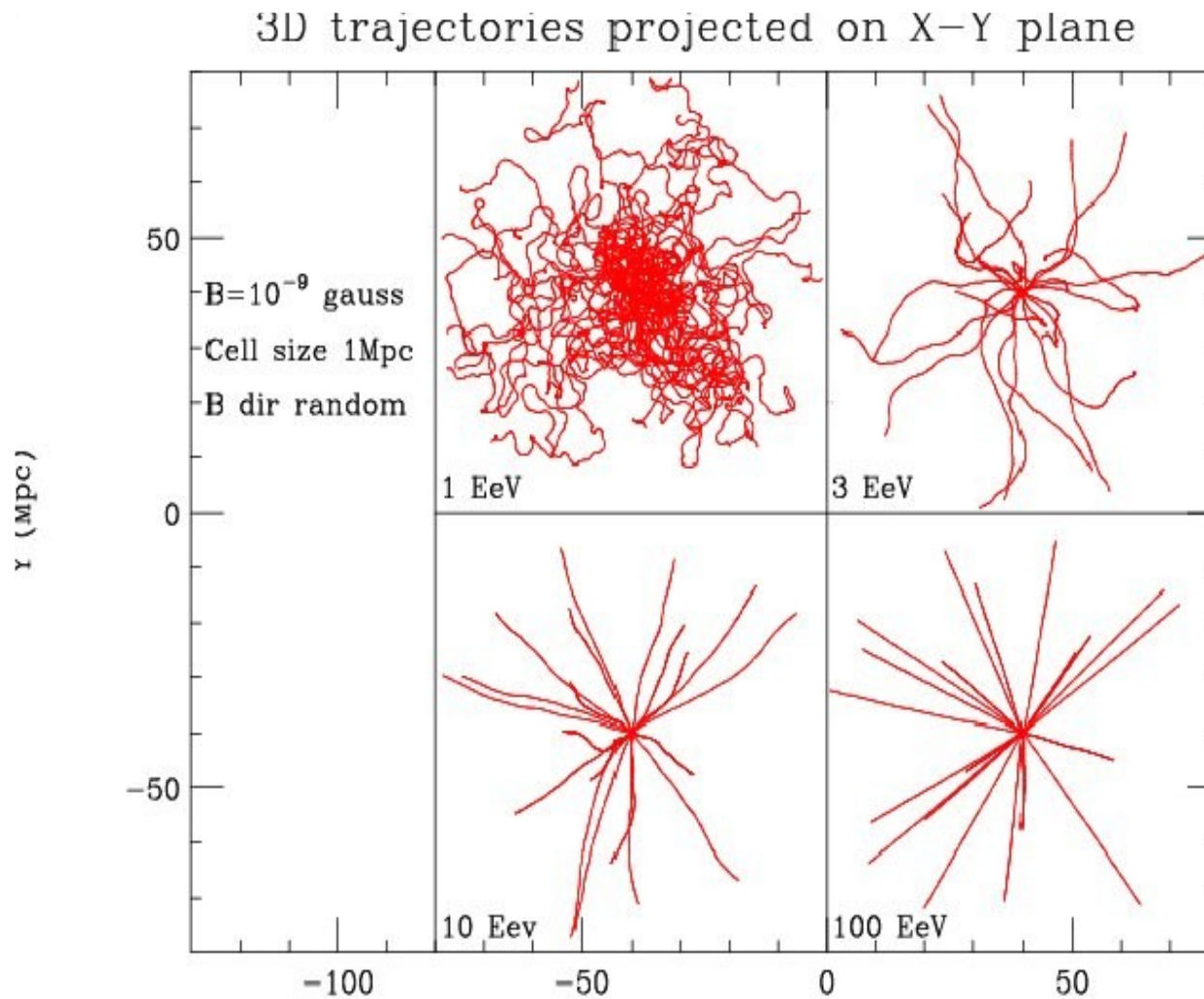


D. Hooper et al.  
Astropart.Phys. 27 (2007), 199

Protons with energies above  $6 \cdot 10^{19}$  eV interact with the microwave background radiation and they rapidly lose energy (GZK cutoff)



# Cosmic rays with energies above $10^{20}$ eV point back to their sources



# Auger science case

*Based on the first Auger ICRC proceedings  
M. Boratav et al, ICRC 1997, Durban*

“The Pierre Auger Observatory...employing a giant array of **particle counters and an optical fluorescence detector**...aims at studying, with high statistics, cosmic rays with energies around and above the so-called Greisen-Zatsepin-Kuzmin spectral cutoff...Its main aims are:...

- a precise reconstruction of the **energy spectrum**...
- the **identification of primaries**, even if only statistical...Are they protons, nuclei, or perhaps something exotic? (e.g., the detection of a large amount of gammas and neutrinos would be an indication in favor of “exotic” theories...)...Inferences on mass composition will be drawn from the study of shower properties that might constrain hadronic interaction models at energies well beyond the reach of accelerator-based experiments...
- a **systematic study of the arrival directions**, that will indicate if there is anisotropy in the distribution and/or clusters which would indicate the existence of point sources...”



# Auger science case

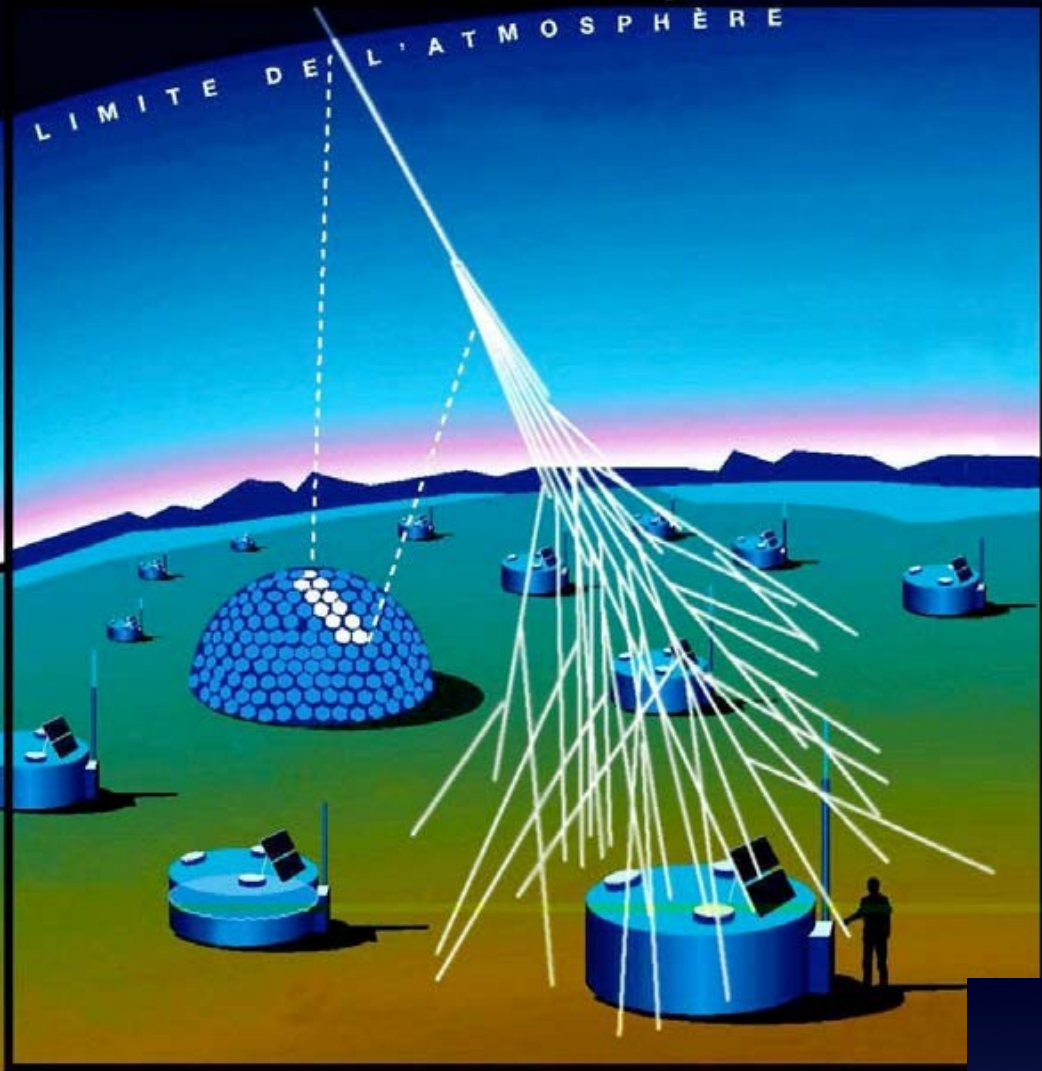
*Based on the first Auger ICRC proceedings  
M. Boratav et al, ICRC 1997, Durban*

“The Pierre Auger Observatory...employing a giant array of **particle counters and an optical fluorescence detector**...aims at studying, with high statistics, cosmic rays with energies around and above the so-called Greisen-Zatsepin-Kuzmin spectral cutoff...Its main aims are:...

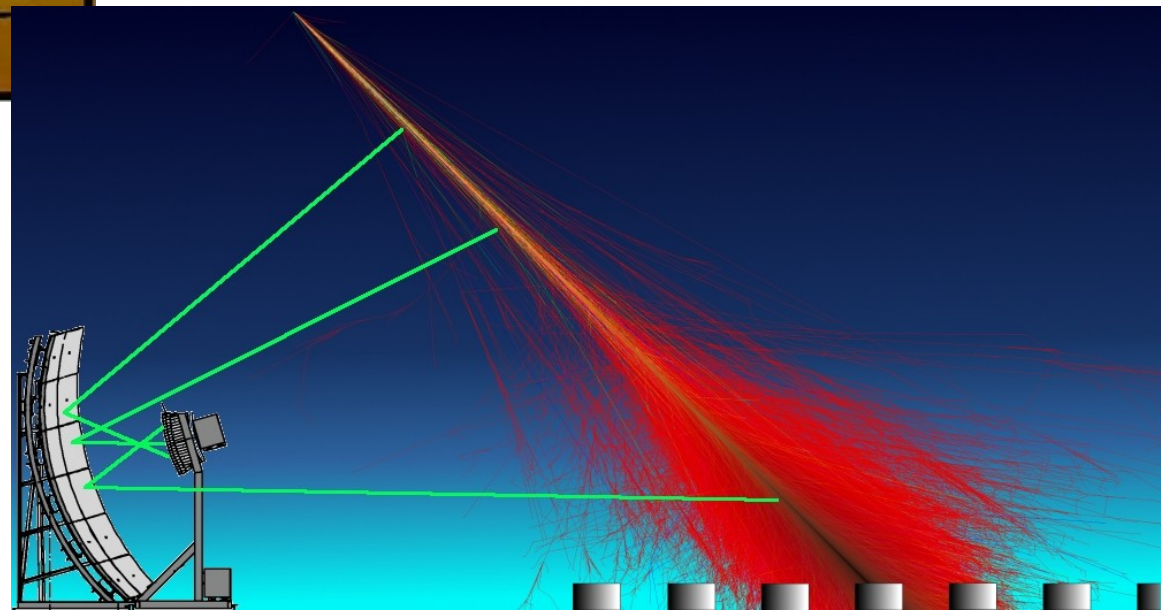
- a precise reconstruction of the **energy spectrum**...
- the **identification of primaries**, even if only statistical...Are they protons, nuclei, or perhaps something exotic? (e.g., the detection of a large amount of gammas and neutrinos would be an indication in favor of “exotic” theories...)...Inferences on mass composition will be drawn from the study of shower properties that **might constrain hadronic interaction models at energies well beyond the reach of accelerator-based experiments**...
- a **systematic study of the arrival directions**, that will indicate if there is anisotropy in the distribution and/or clusters which would indicate the existence of point sources...”

# The Pierre Auger Collaboration





**“The Pierre Auger Observatory...employing a giant array of particle counters and an optical fluorescence detector...is a “hybrid” ground detector...”**

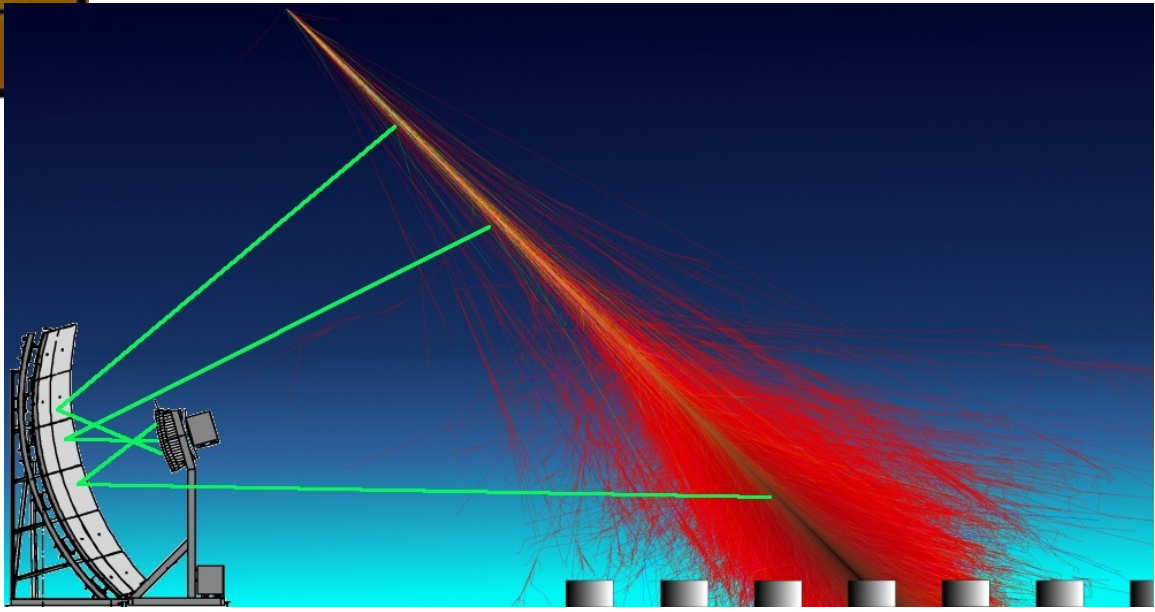




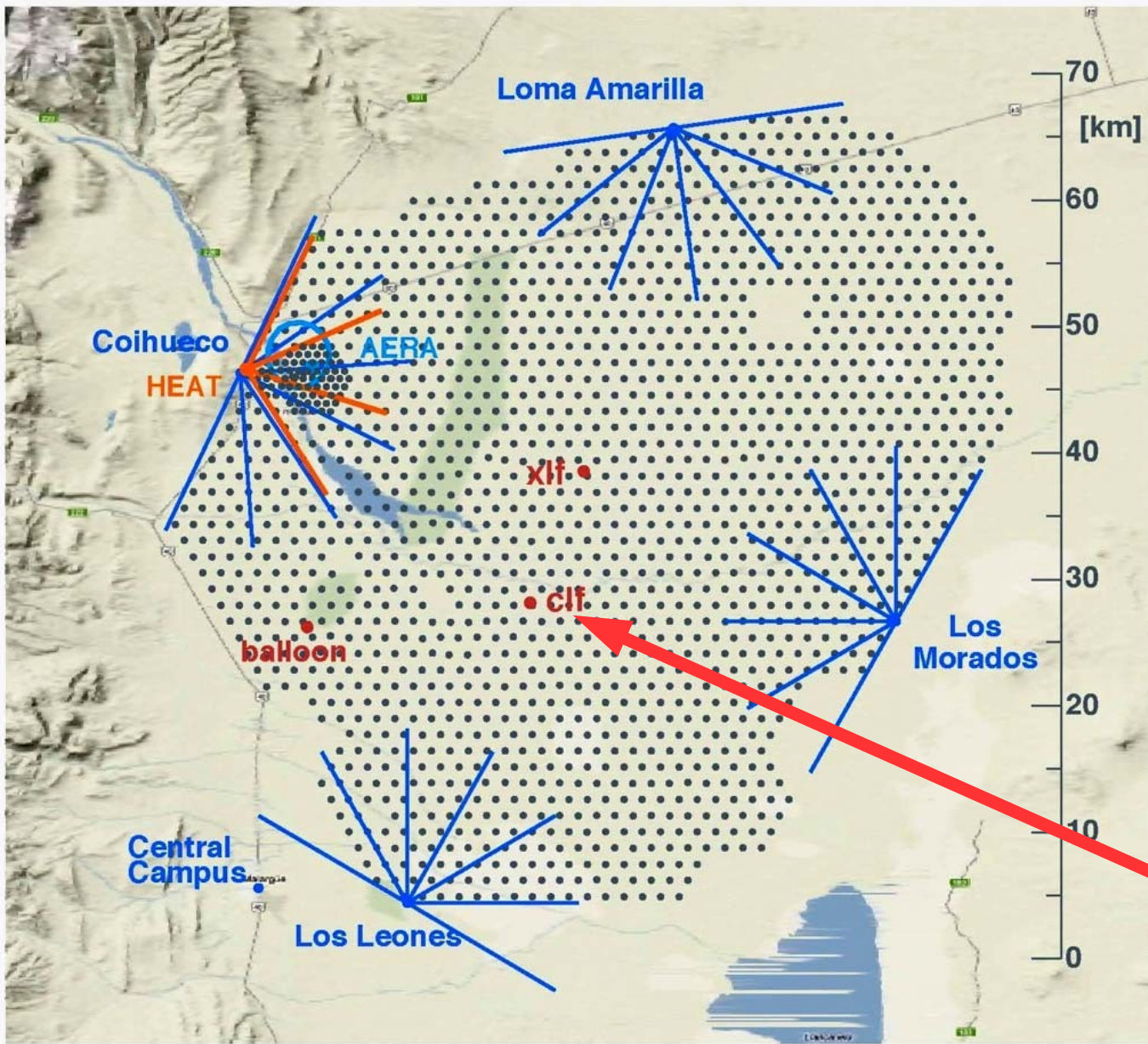
**“The Pierre Auger Observatory...employing a giant array of particle counters and an optical fluorescence detector...is a “hybrid” ground detector...”**

**Surface Detector (SD)**

**Fluorescence Detector (FD)**

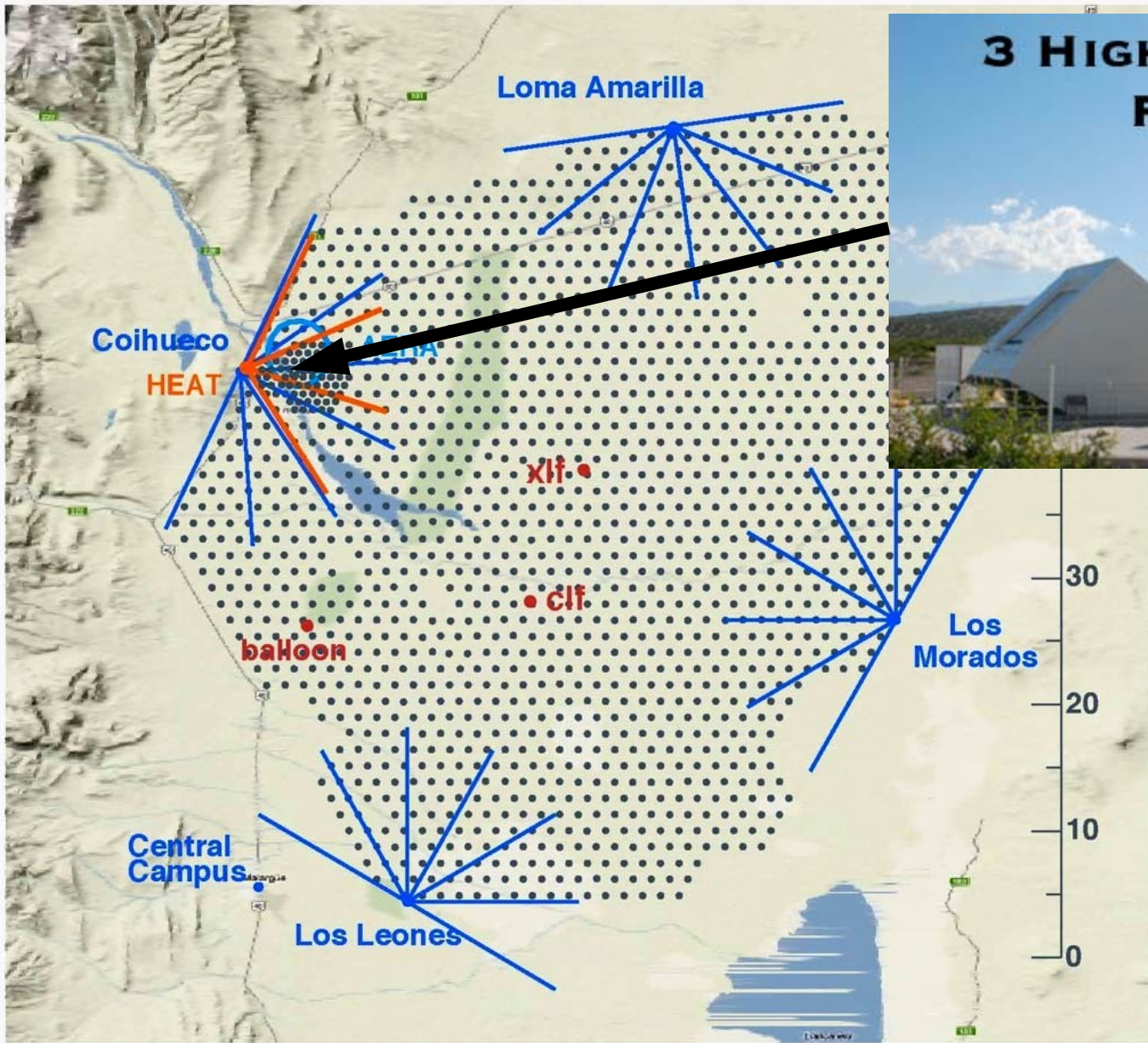


# The Pierre Auger Observatory, Argentina



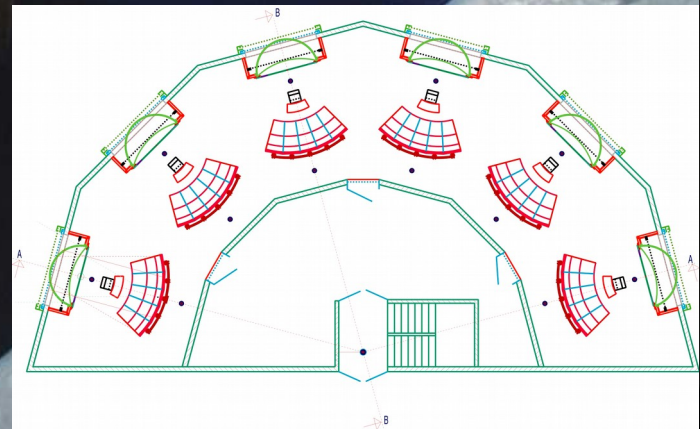
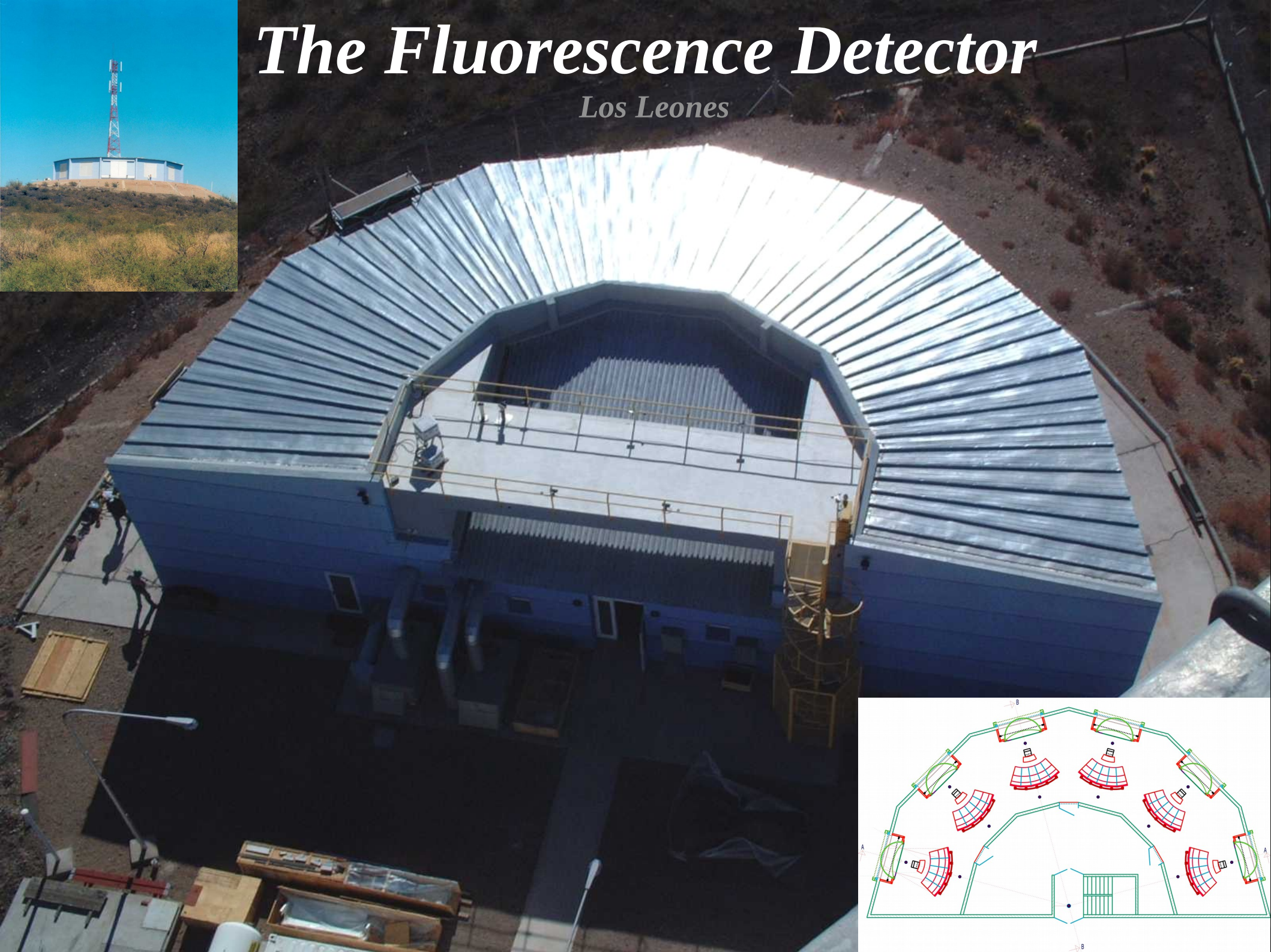
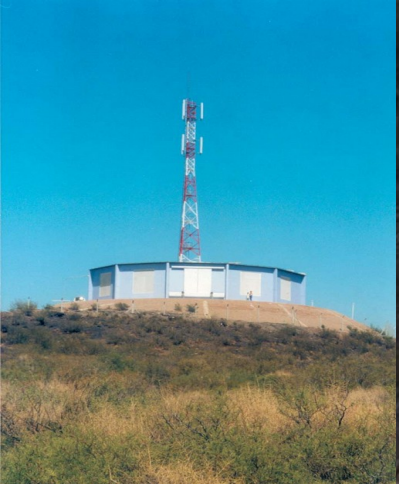
# The Pierre Auger Observatory, Argentina

## HEAT

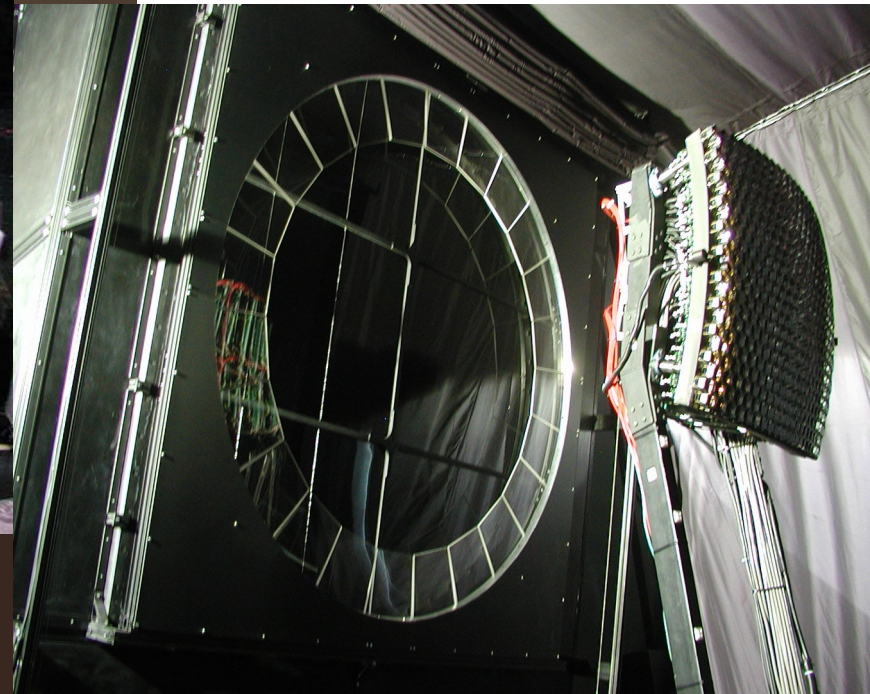
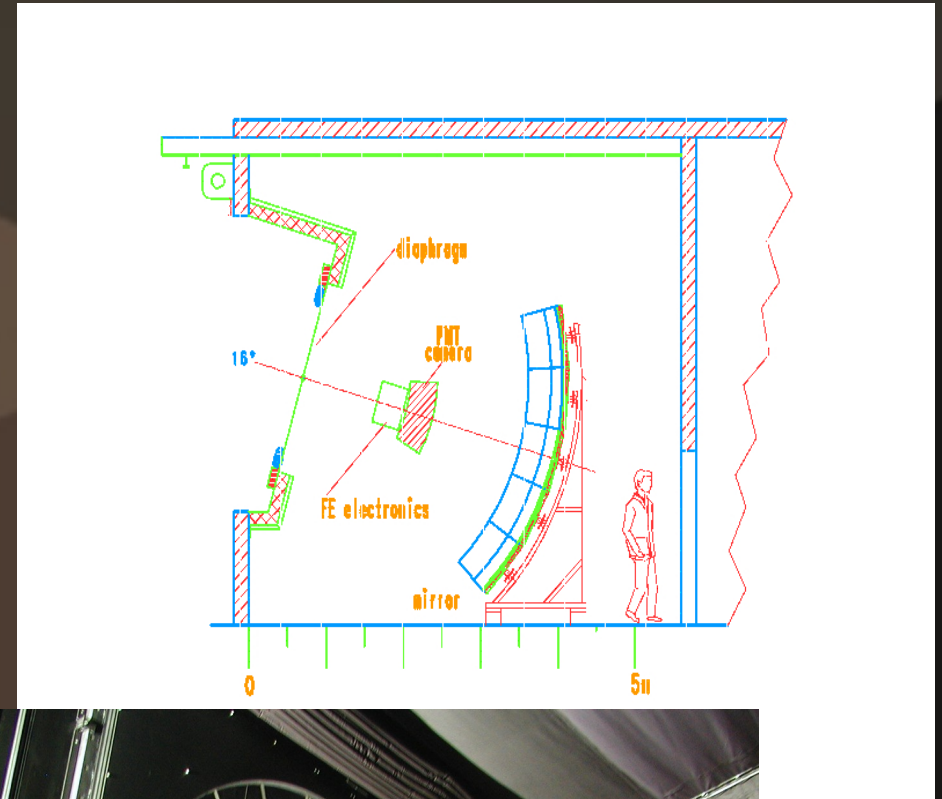
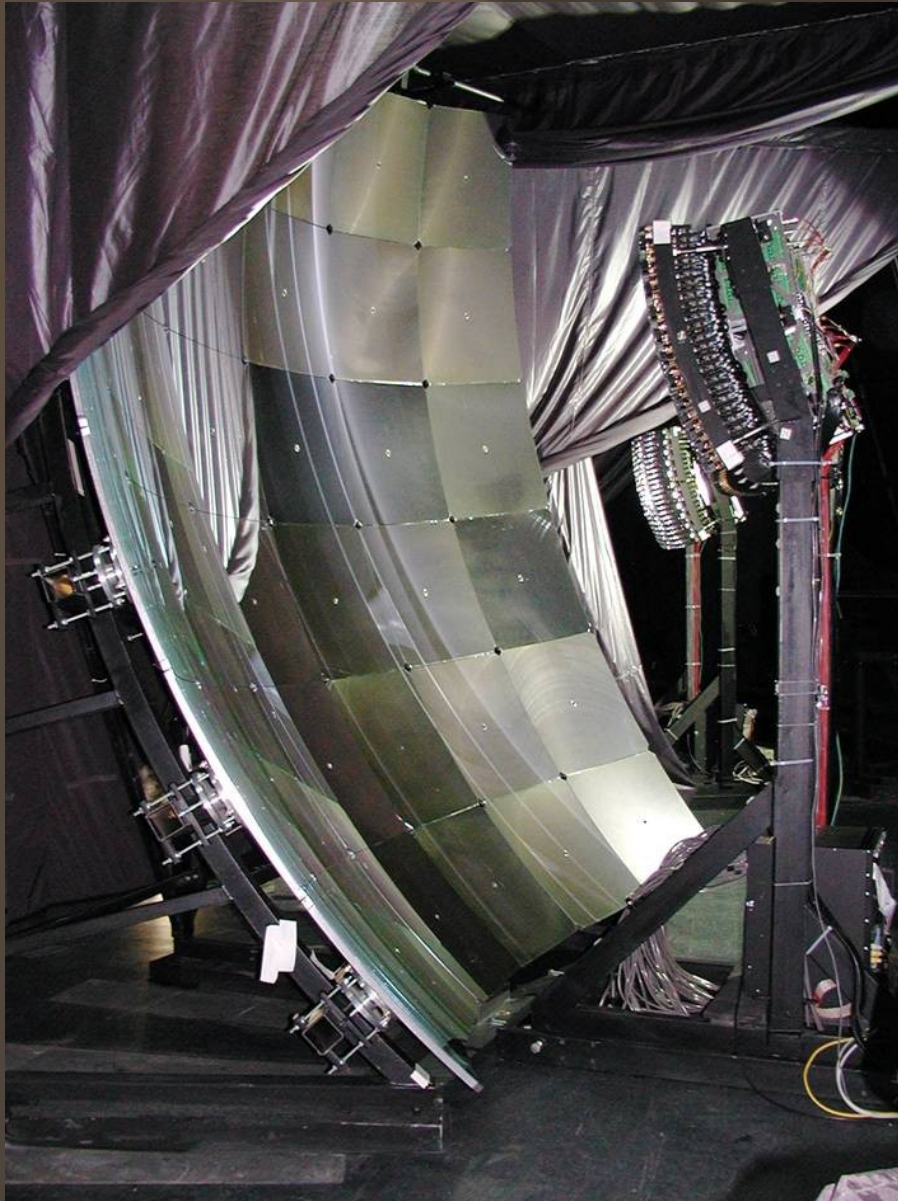


# *The Fluorescence Detector*

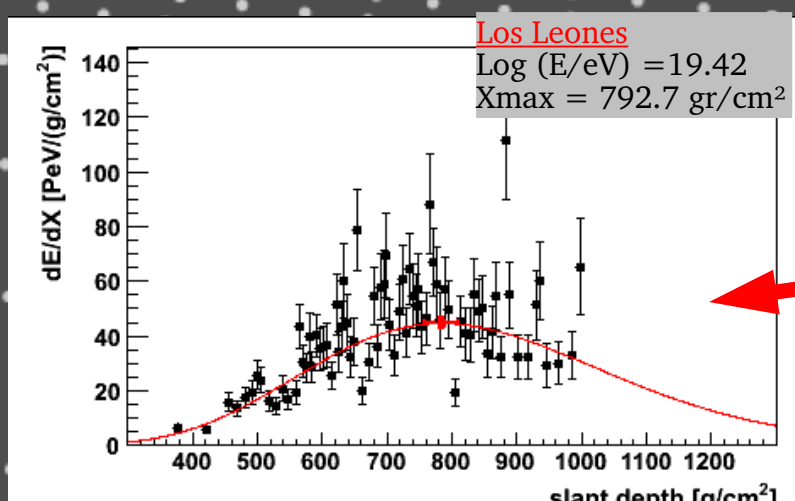
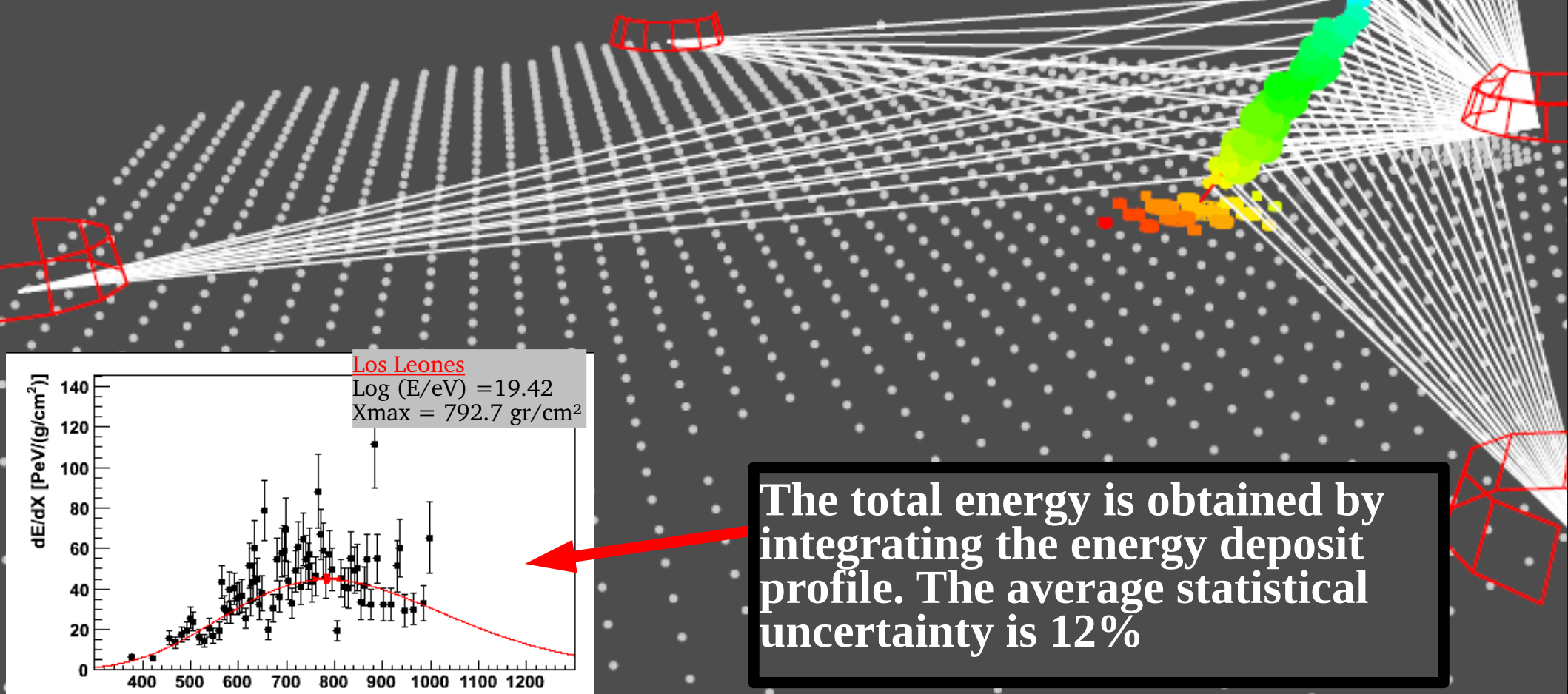
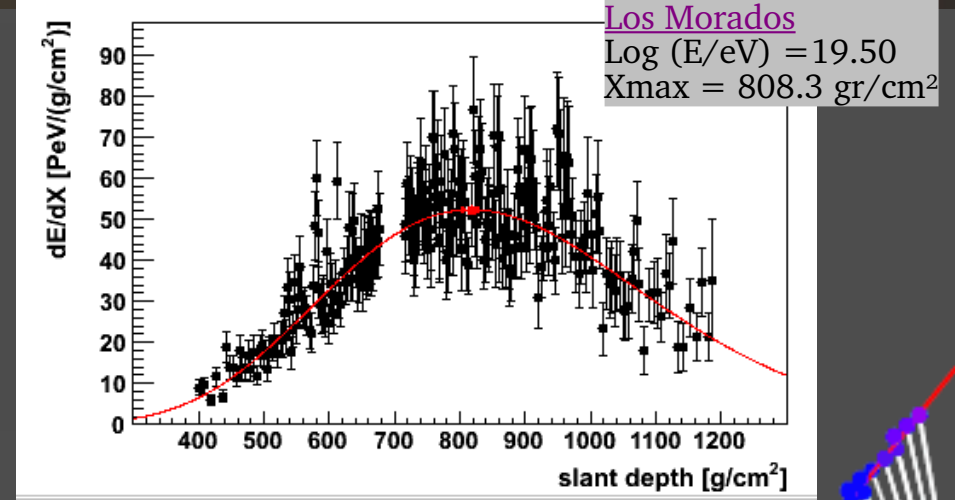
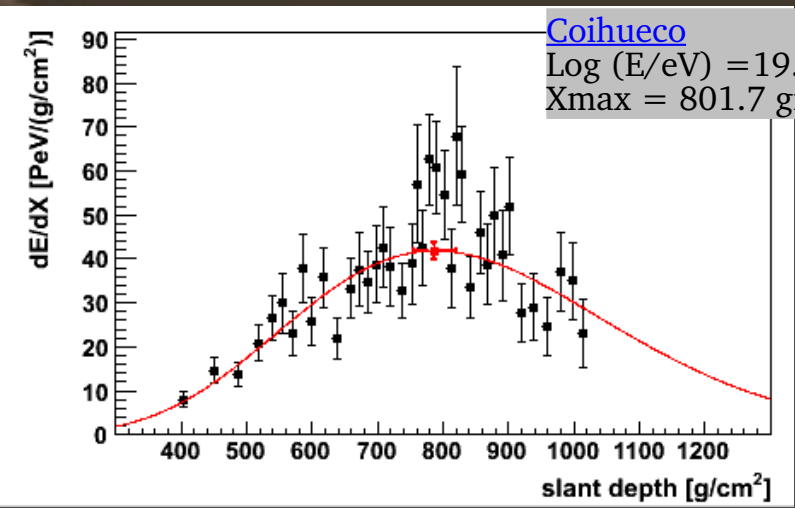
*Los Leones*



# The Fluorescence Detector







The total energy is obtained by integrating the energy deposit profile. The average statistical uncertainty is 12%

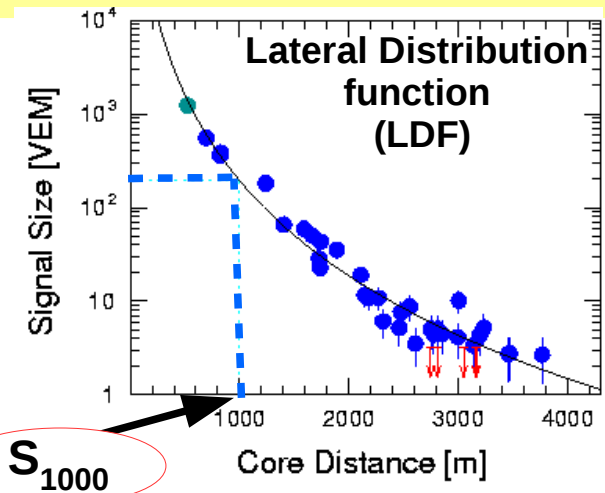
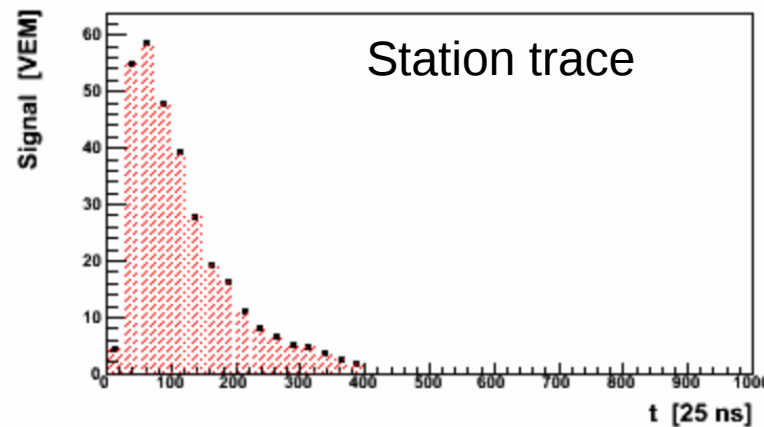
# Event Reconstruction

## Arrival direction, energy and mass

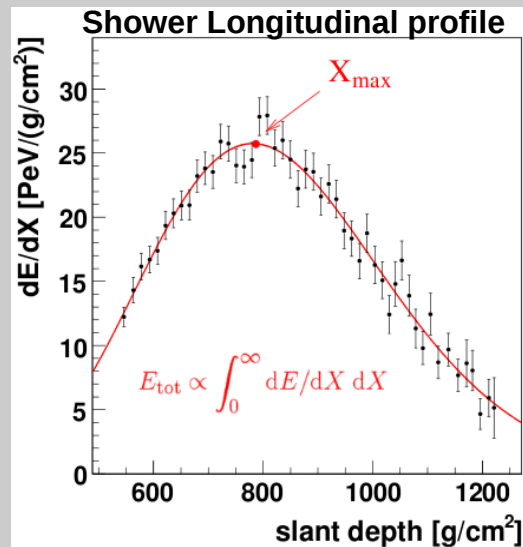
### Geometry (arrival direction)

- from timing and position information of the triggered SD stations.
- For the subset of events that also triggered the FD (hybrid events): from pixel timing, pixel FOV direction and position and timing of only the brightest SD station.

With SD



With FD



The  $X_{max}$  resolution is in average  $20 \text{ g/cm}^2$

Calorimetric metric measurement of the energy

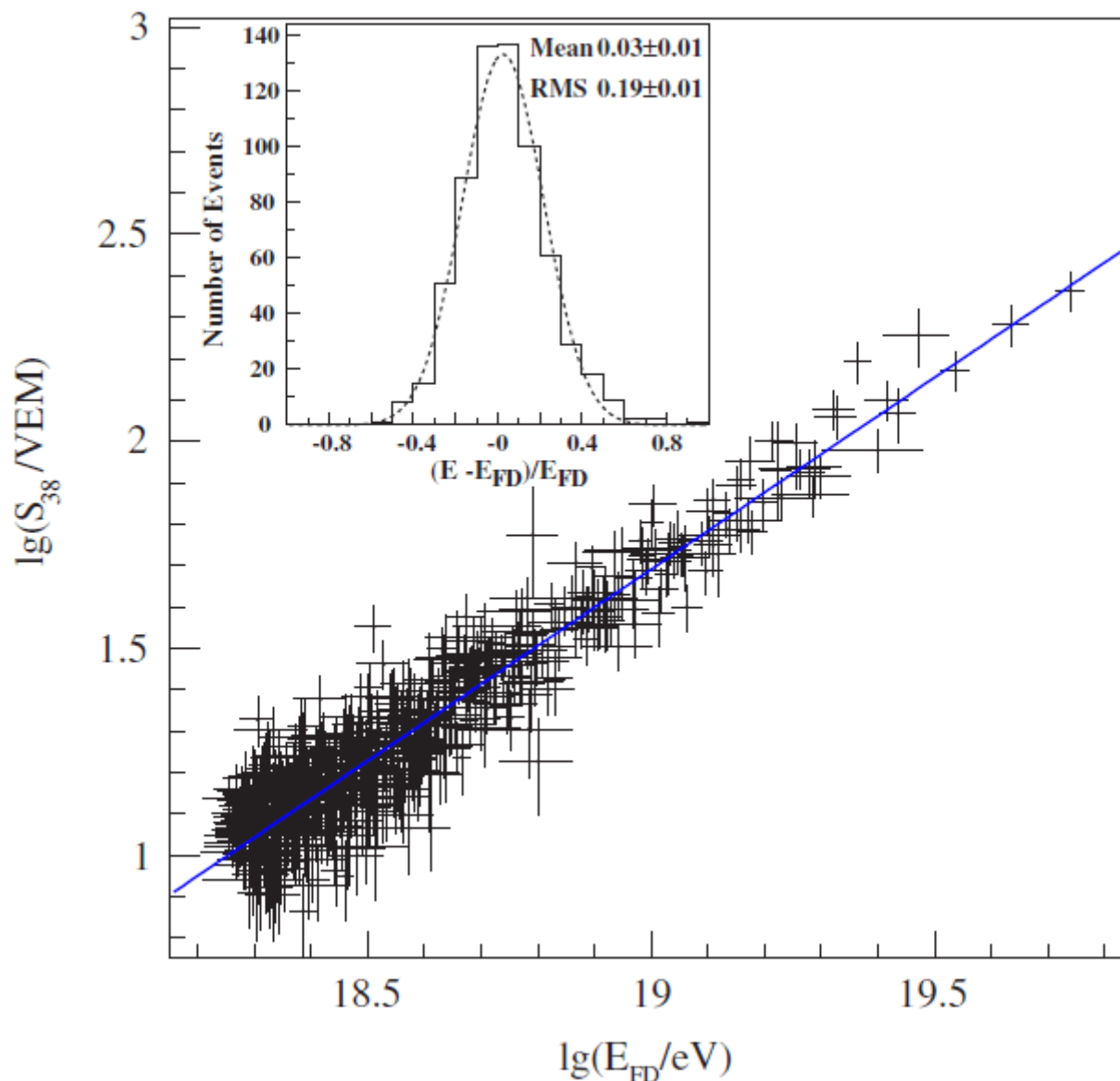
# The Energy scale from the FD is transferred to the SD

The energy converter:

Compare ground parameter  $S(1000)$  with the fluorescence detector energy.

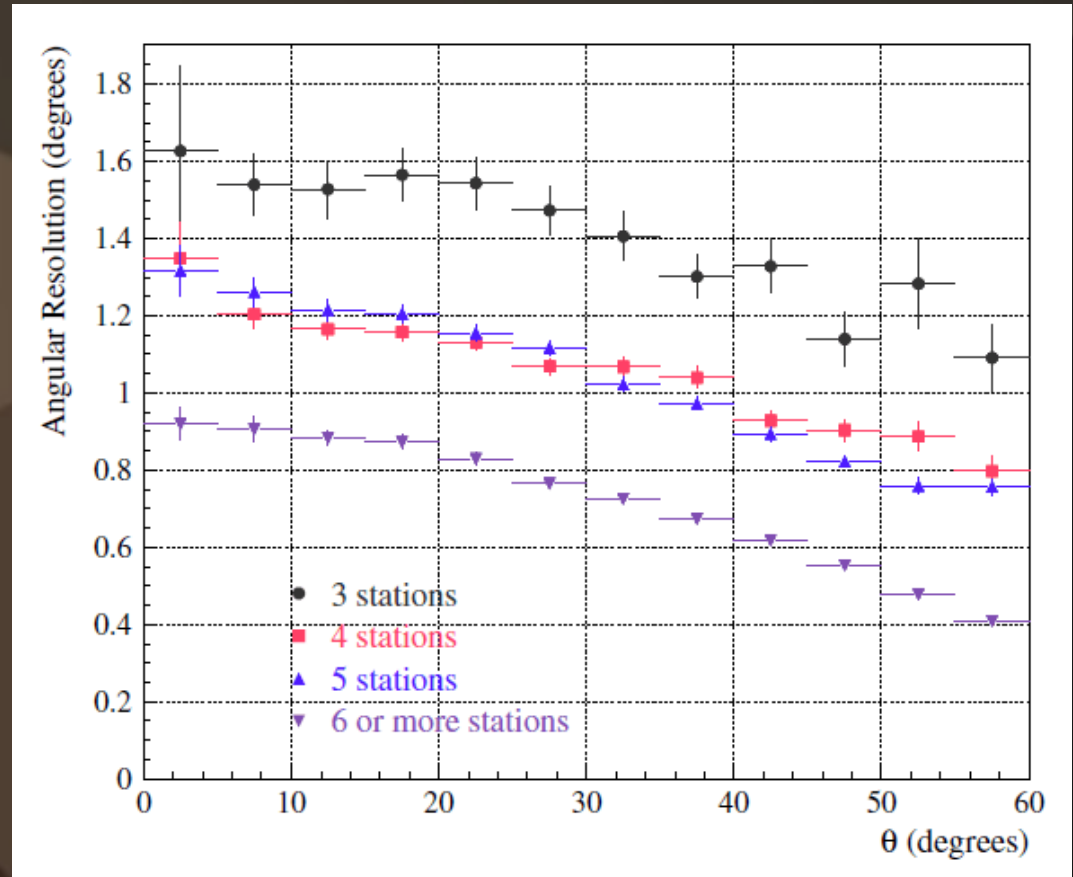
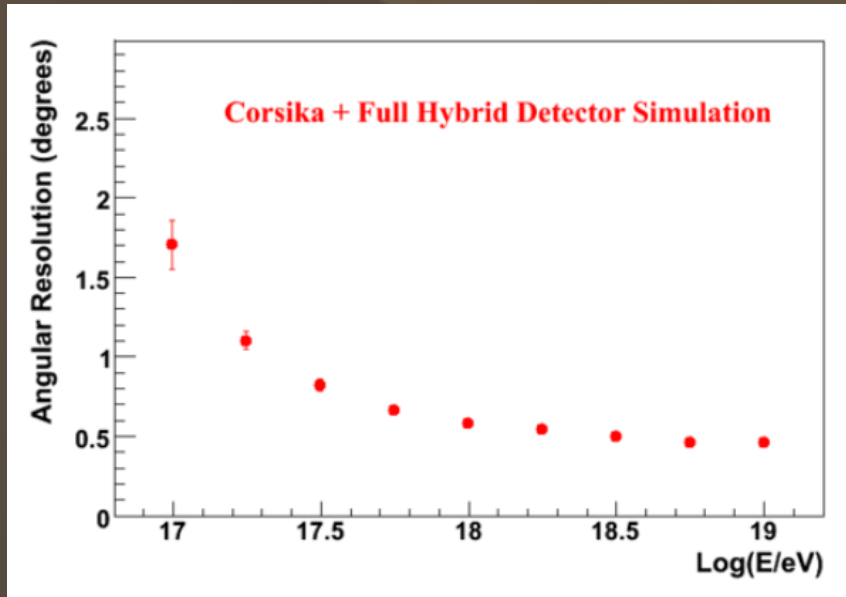
The systematic uncertainties of the fluorescence detector (14%) are transferred to the surface detector.

The surface detector energy resolution is about 20% at the lowest energies and 10% at the highest energies.



**Note:**  $S_{1000}$  for a given shower energy varies depending on the zenith angle. So,  $S_{38}$  is the corresponding expectation for a  $38^\circ$  shower, given the  $S_{1000}$  measurement.

# Angular Resolution

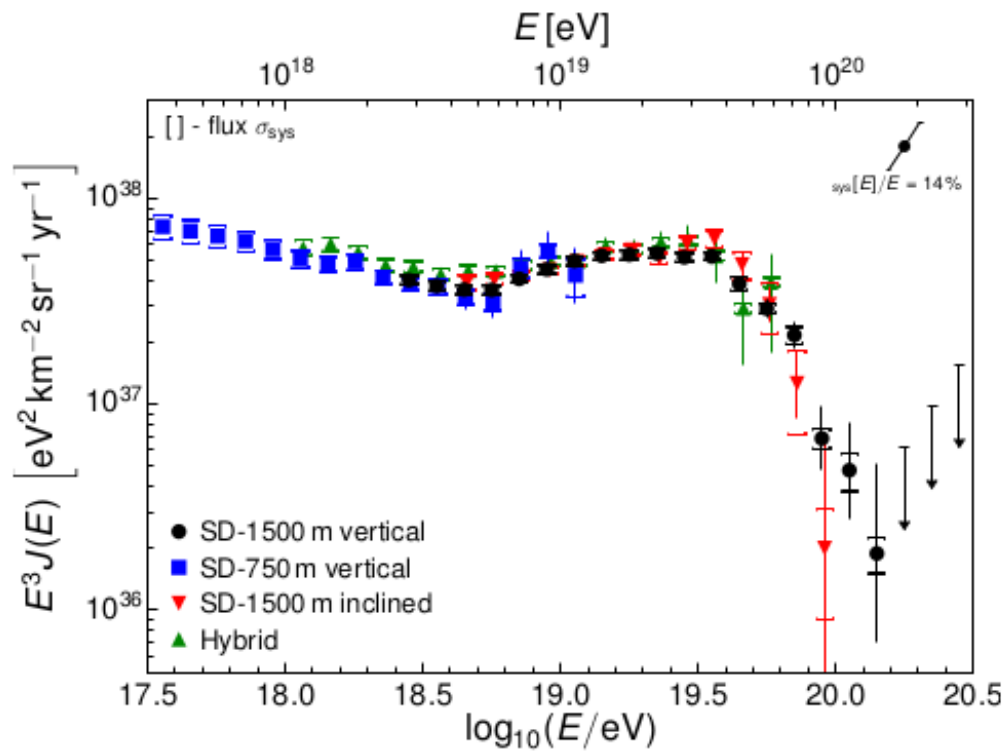


Hybrid Angular resolution  
(68% CL)  
*0.5 degrees above 1EeV*

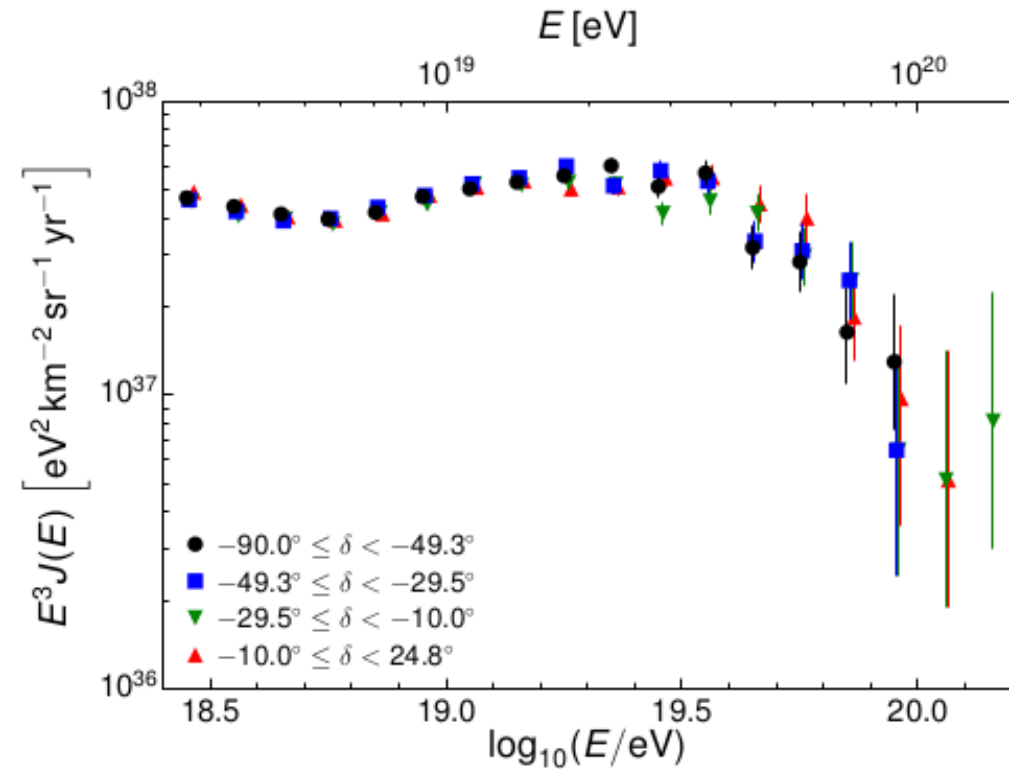
Surface array Angular resolution (68% CL)  
**< 1.6° for 3 station events ( $E > 3EeV, \theta < 60^\circ$ )**  
**< 1.2° for 4 station events**  
**< 0.9° for 6 or more station events**

# The Cosmic Ray Energy Spectrum

Four independent measurements

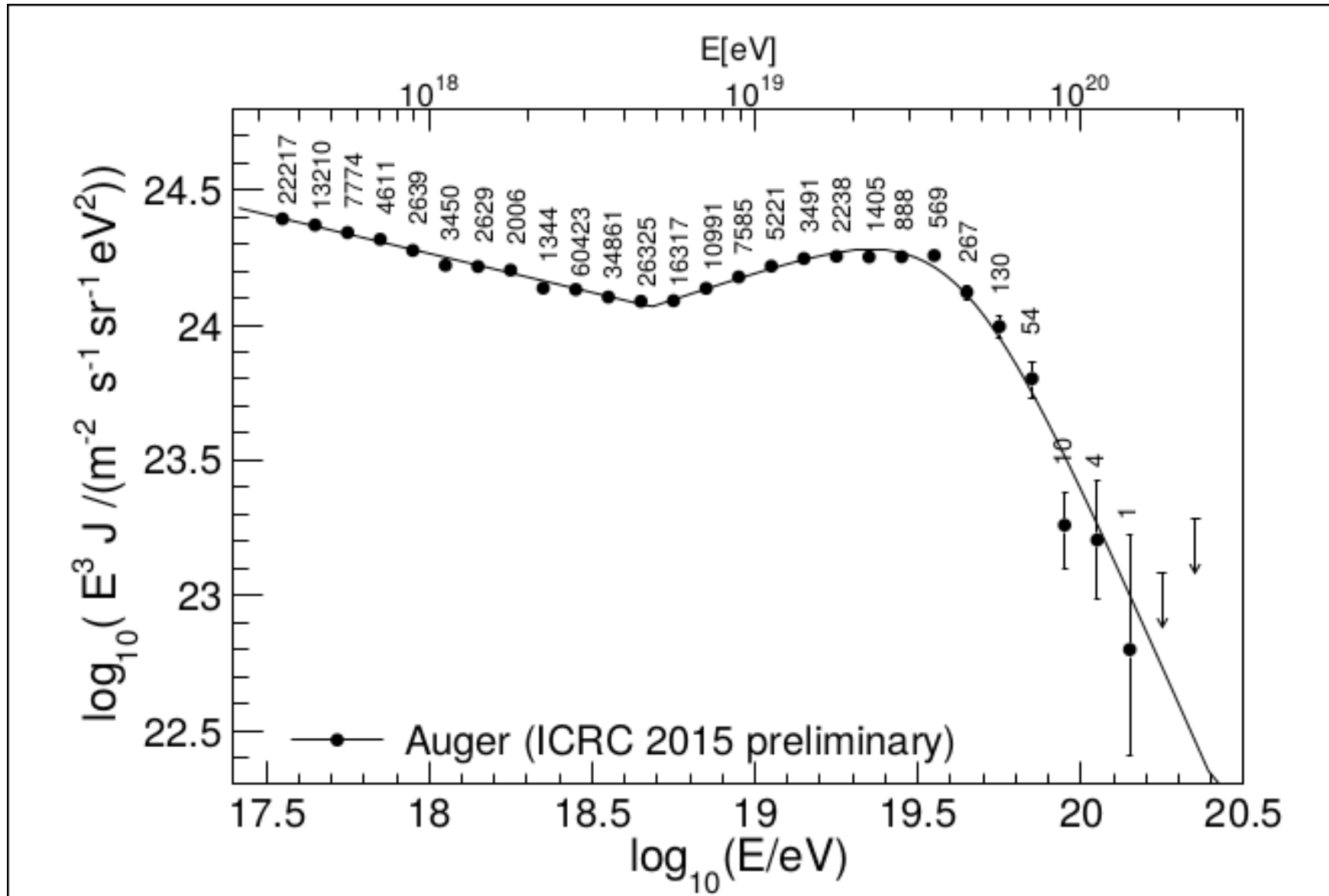


Declination dependence



# The Cosmic Ray Energy Spectrum

(combining all measurements)



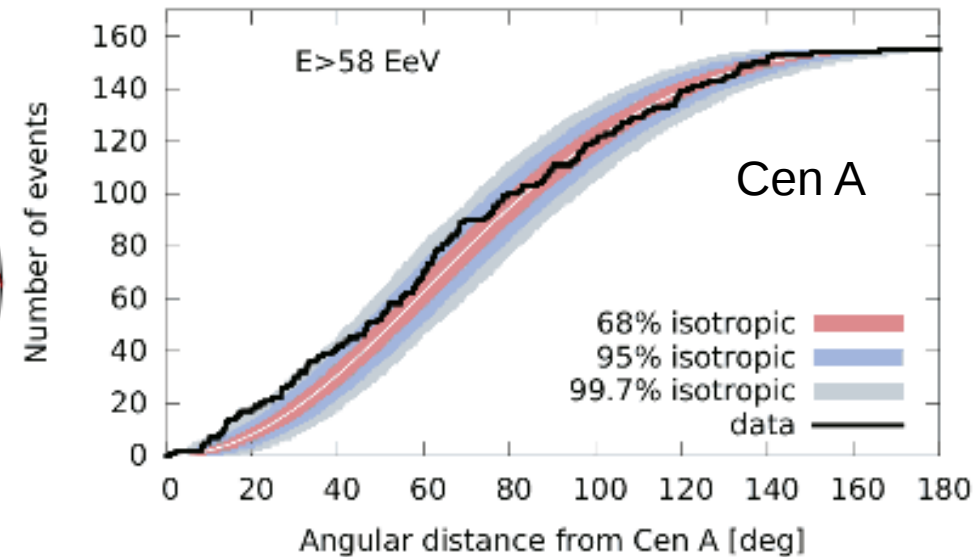
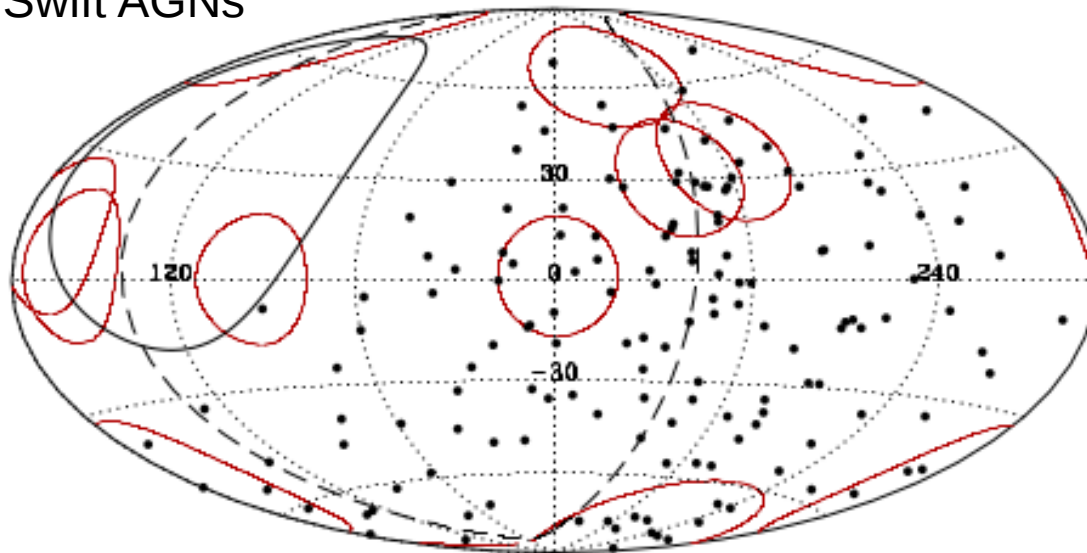
# Arrival Directions

## Cross correlation studies

Objects	$E_{\text{th}}$ [EeV]	$\Psi$ [ $^{\circ}$ ]	$D$ [Mpc]	$\mathcal{L}_{\text{min}}$ [erg/s]	$f_{\text{min}}$	$\mathcal{P}$
2MRS Galaxies	52	9	90	-	$1.5 \times 10^{-3}$	24%
Swift AGNs	58	1	80	-	$6 \times 10^{-5}$	6%
Radio galaxies	72	4.75	90	-	$2 \times 10^{-4}$	8%
Swift AGNs	58	18	130	$10^{44}$	$2 \times 10^{-6}$	1.3%
Radio galaxies	72	4.75	90	$10^{39.33}$	$5.1 \times 10^{-5}$	11%
Centaurus A	58	15	-	-	$2 \times 10^{-4}$	1.4%

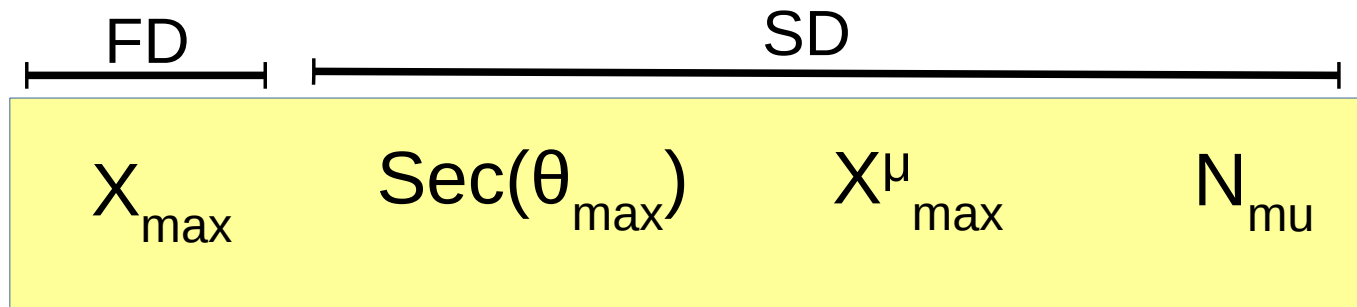
**Table 1:** Summary of the parameters of the minima found in the cross-correlation analyses.

## Swift AGNs



Map in galactic coordinates

## Auger measurements related to mass composition



Correlation factor between:

$X_{\max}$  and  $S_{1000}$

(Hybrid events)



PHYSICAL REVIEW D **90**, 122005 (2014)

**Depth of maximum of air-shower profiles at the Pierre Auger Observatory. I. Measurements at energies above  $10^{17.8}$  eV**

$X_{\max}$

PHYSICAL REVIEW D **90**, 122006 (2014)

PHYSICAL REVIEW D **93**, 072006 (2016)

**Azimuthal asymmetry in the risetime of the surface detector signals of the Pierre Auger Observatory**

$\text{Sec}(\theta_{\max})$

PHYSICAL REVIEW D **90**, 012012 (2014)

**Muons in air showers at the Pierre Auger Observatory: Measurement of atmospheric production depth**

$X_{\max}^{\mu}$

PHYSICAL REVIEW D **91**, 032003 (2015)

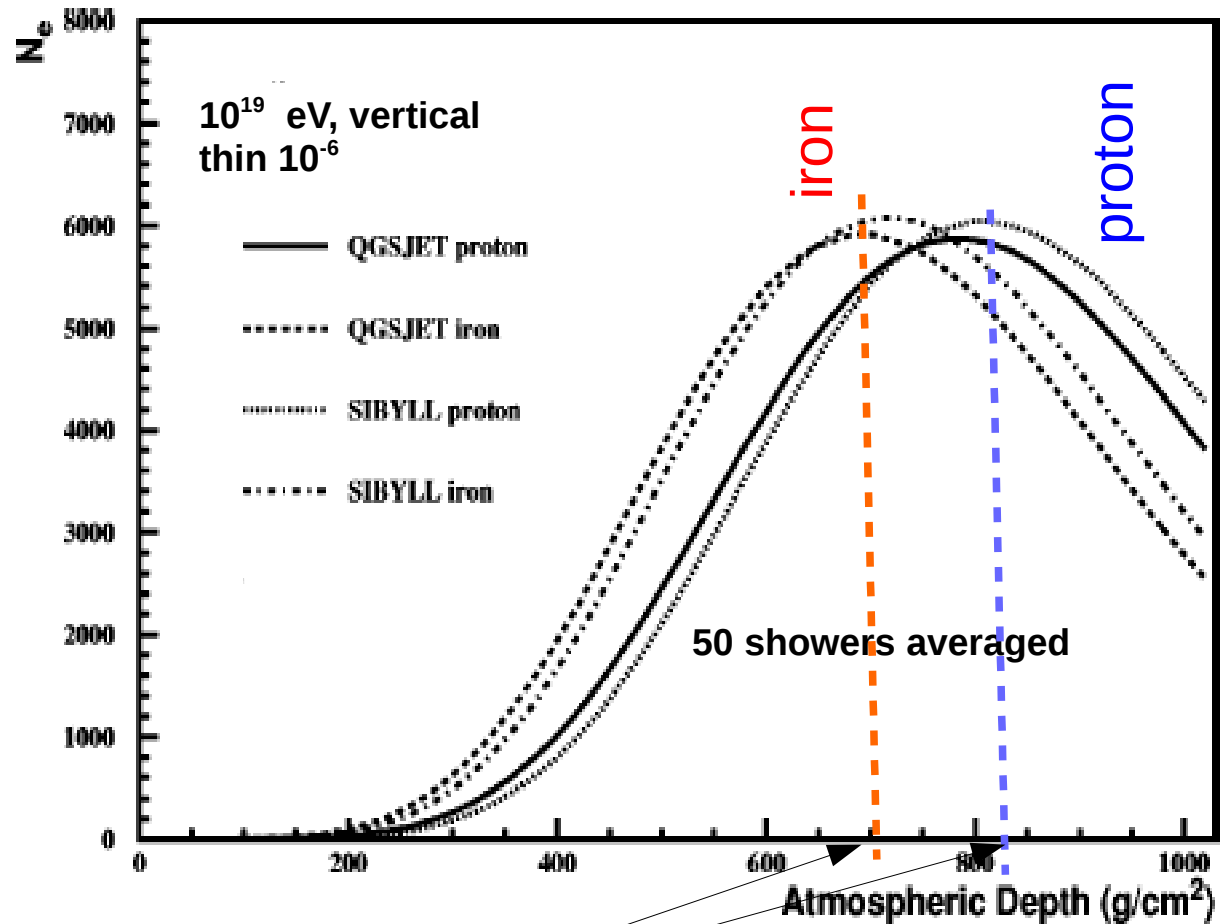


**Muons in air showers at the Pierre Auger Observatory: Mean number in highly inclined events**

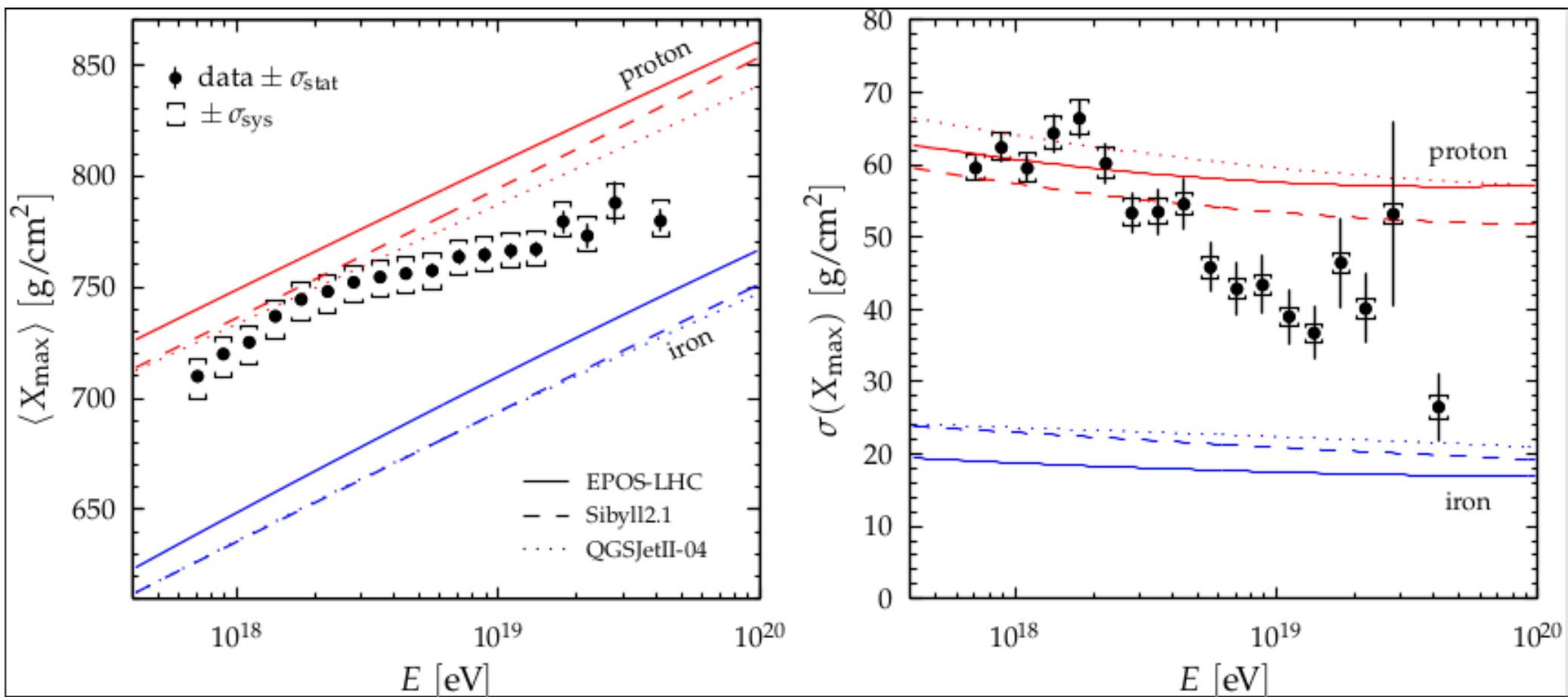
$N_{\mu}$

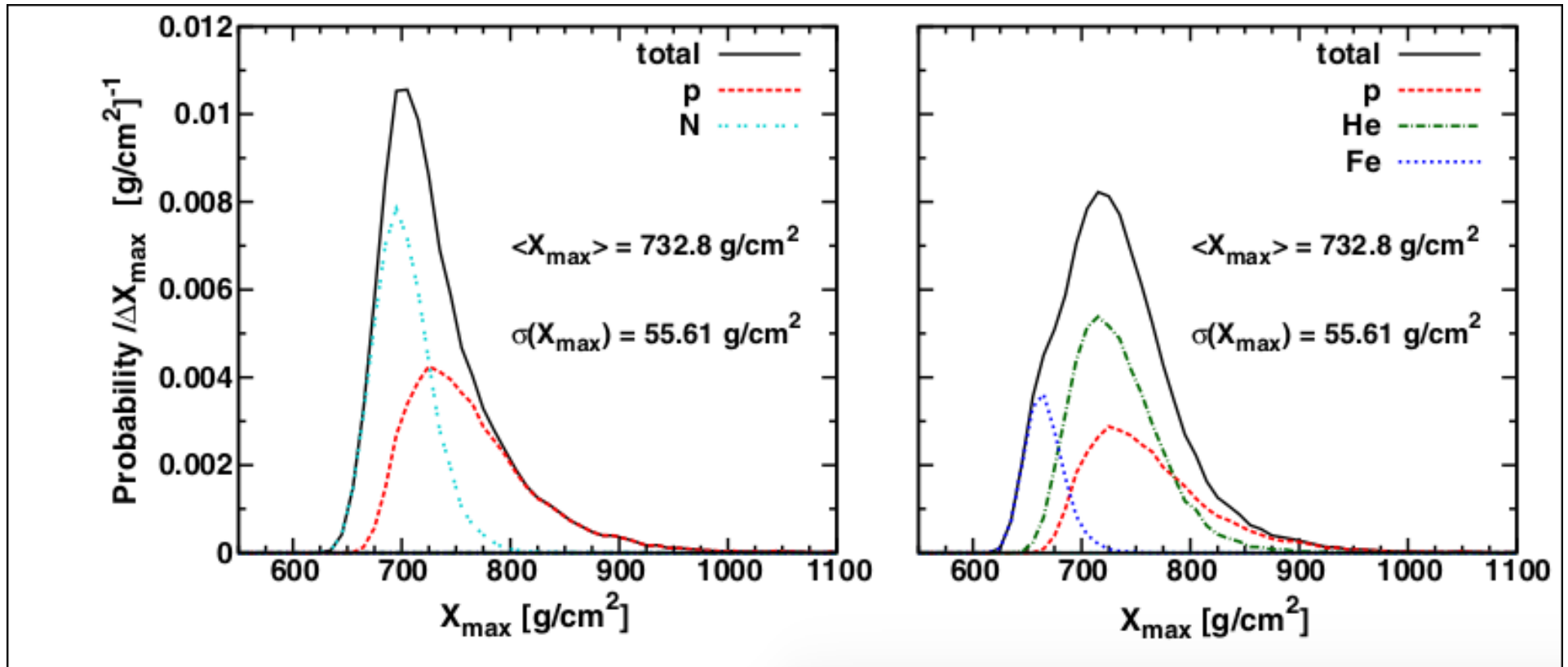
# FD Observables

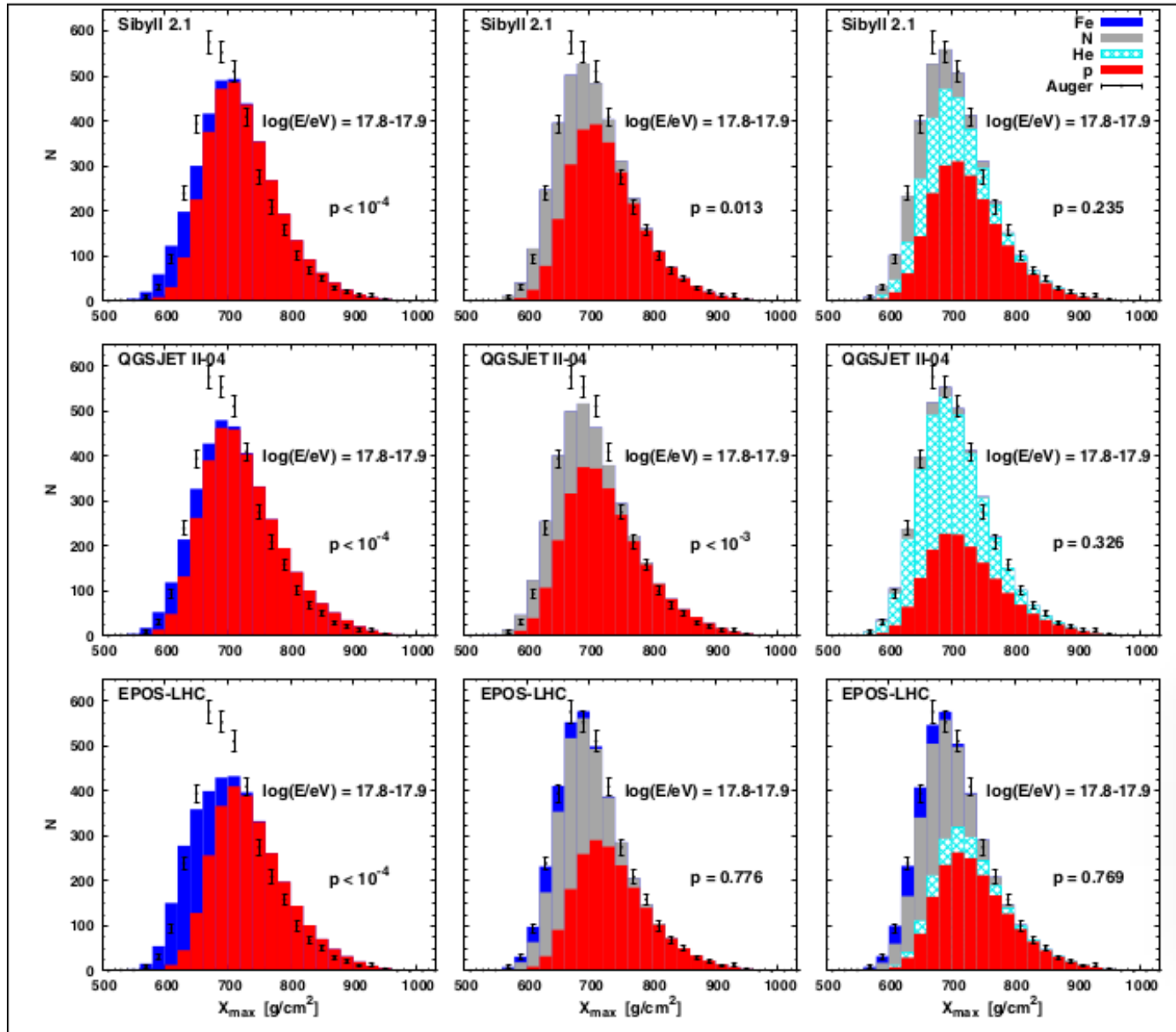
# The expected shower profile (measured by the FD) for proton and Iron are different

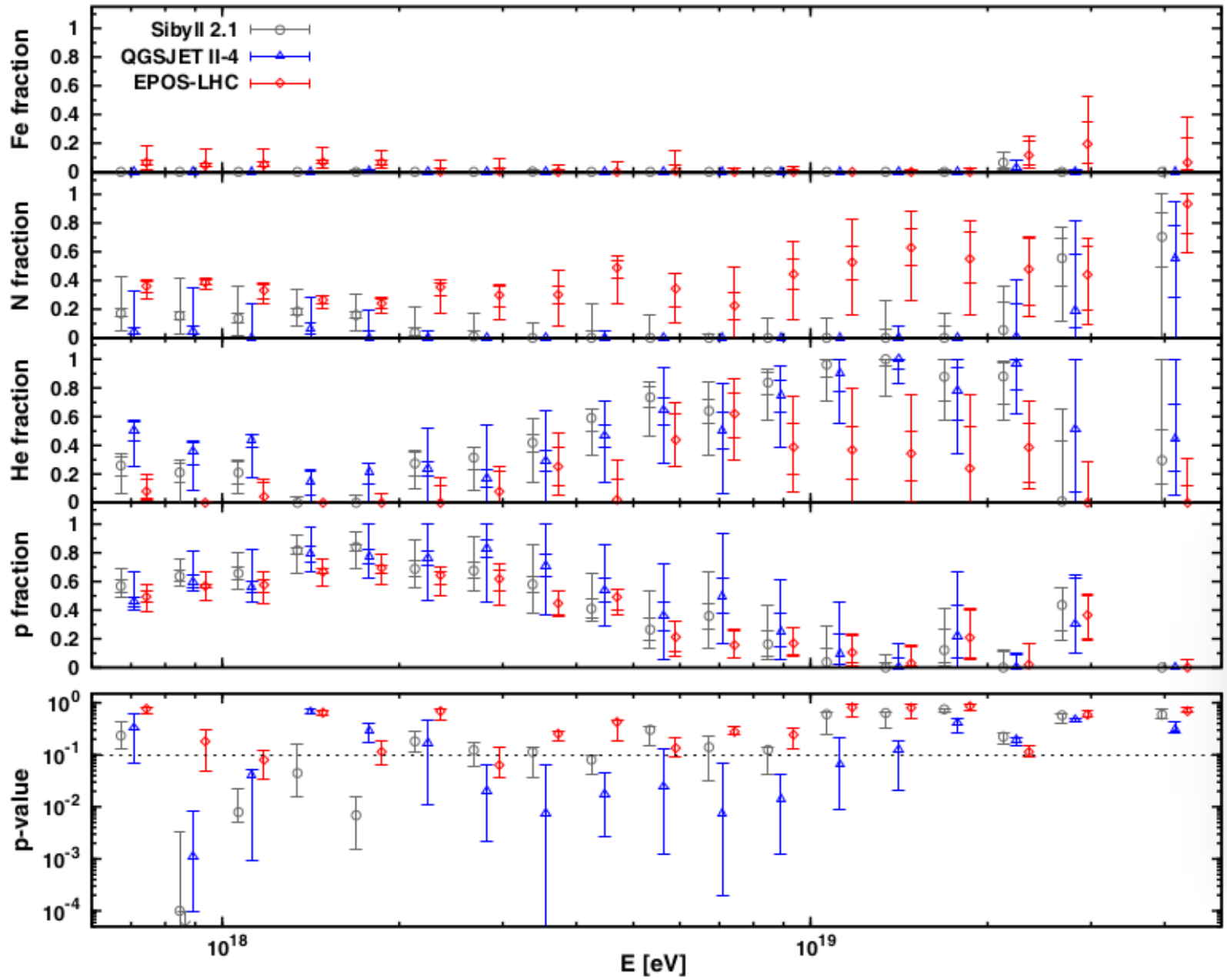


Note:  $X_{\max}$  is used to characterize the shower profile.



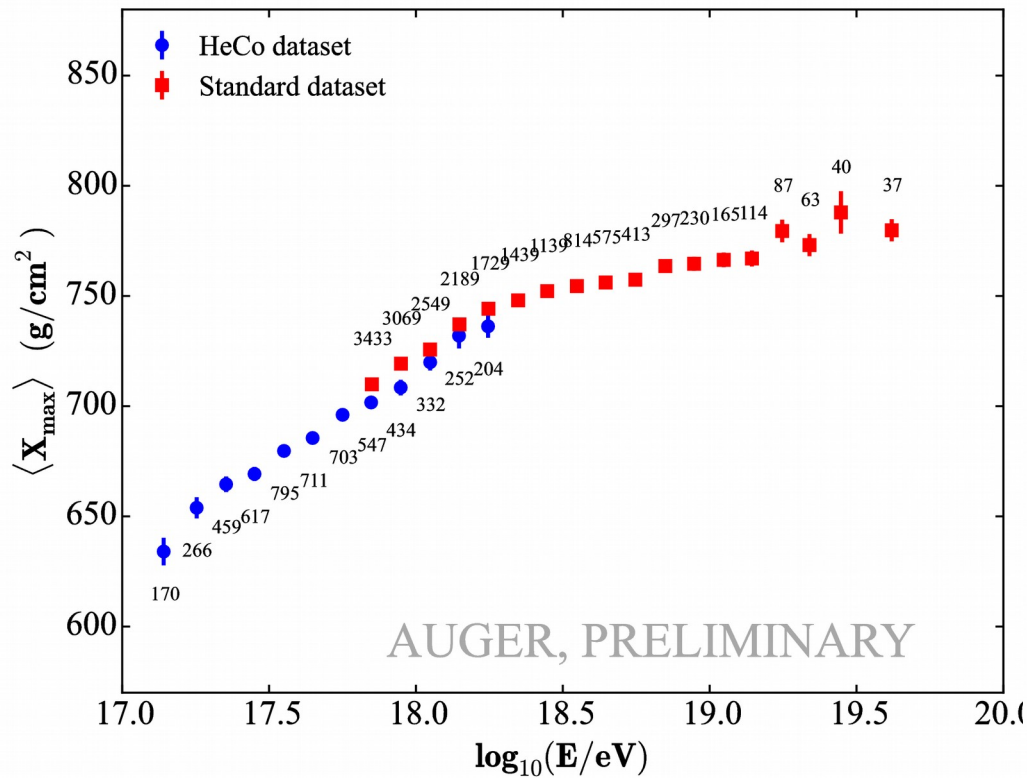




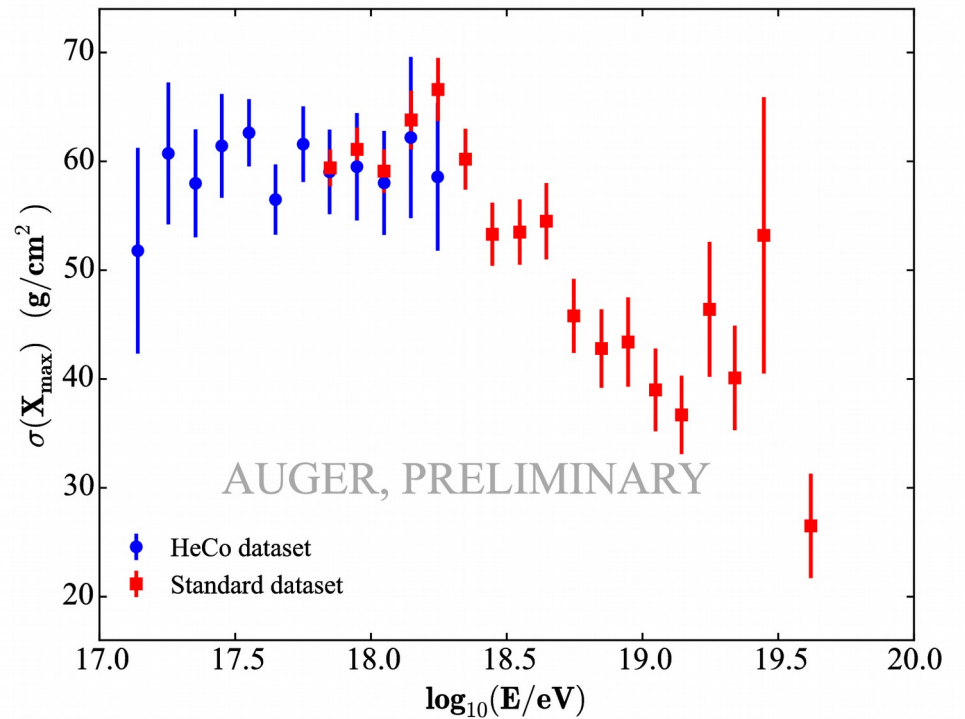


# $X_{\max}$ moments from HEAT and from standard FD measurements

Average of  $X_{\max}$



Std. deviation of  $X_{\max}$

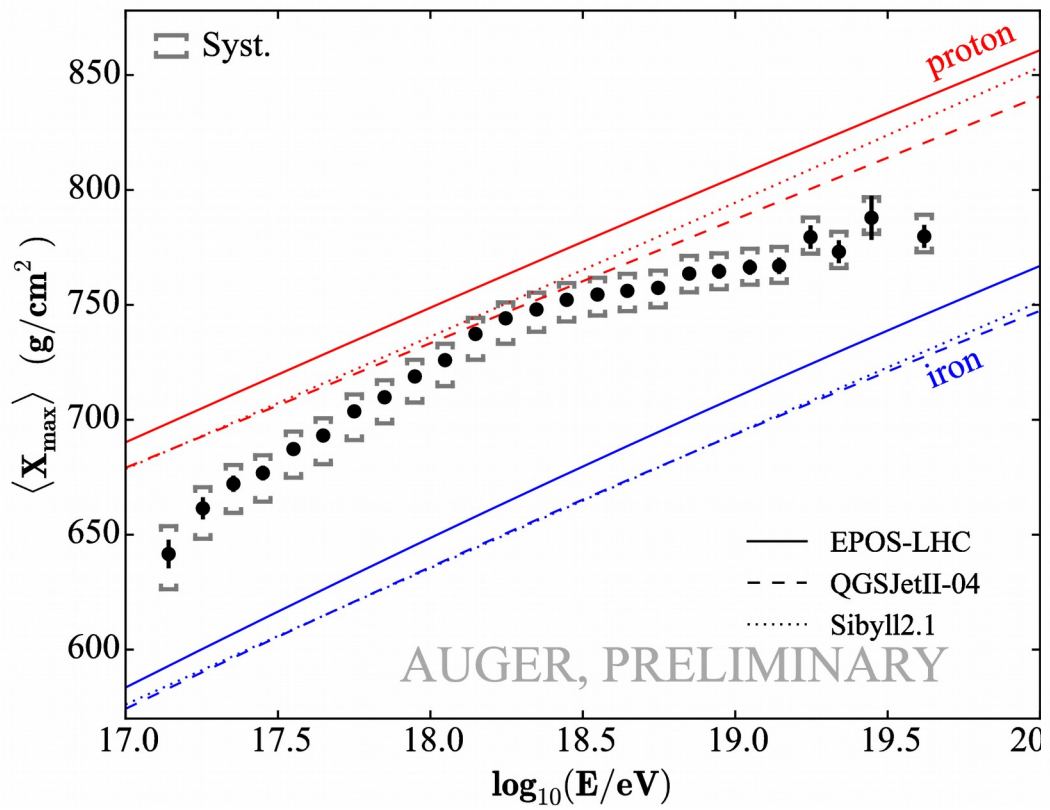


Standard FD  $\rightarrow$  PHYSICAL REVIEW D 90, 122005 (2014)

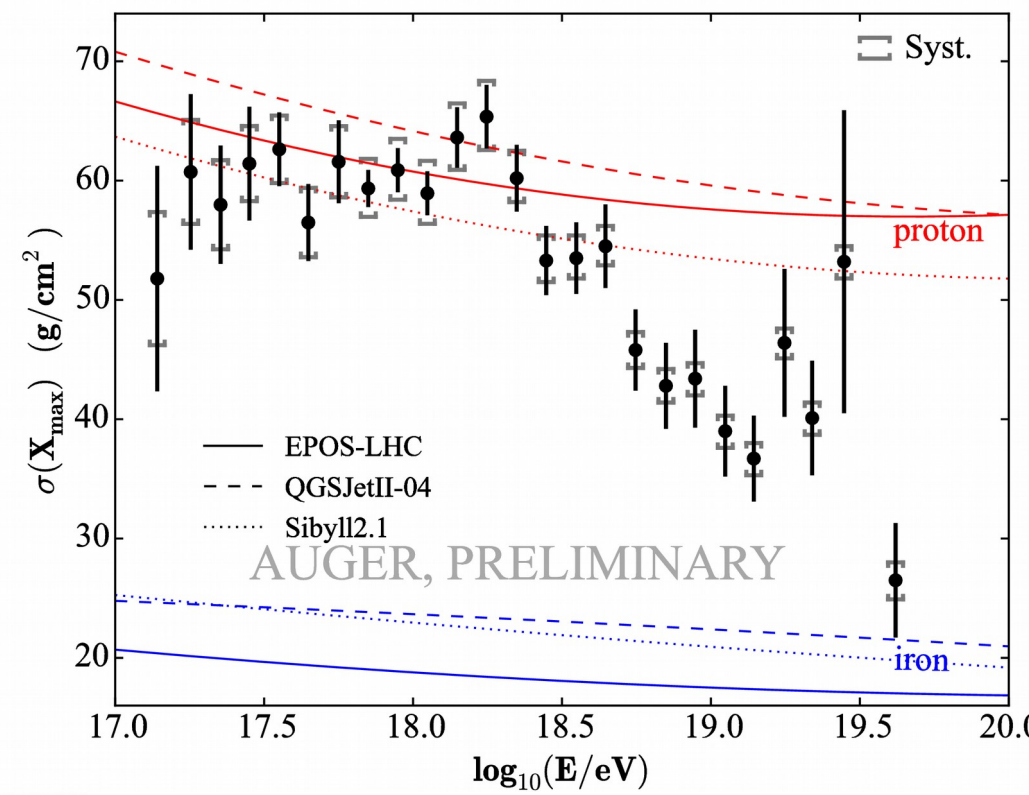


# $X_{\max}$ moments combining HEAT and standard FD measurements

Average of  $X_{\max}$

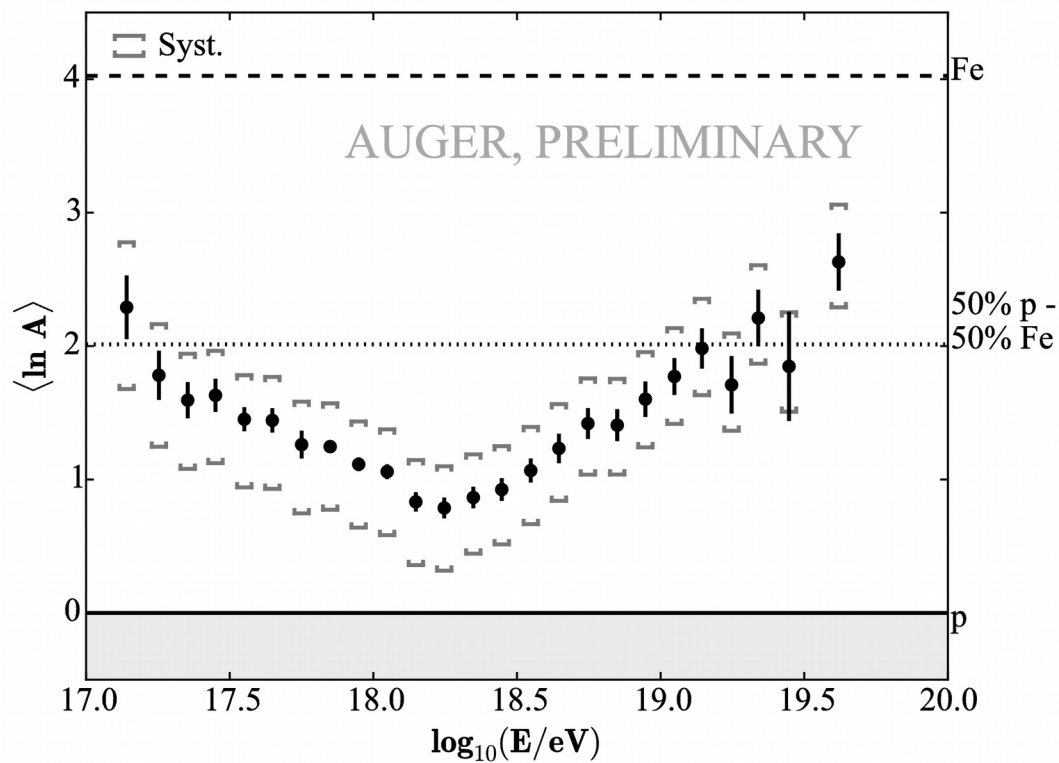


Std. Deviation of  $X_{\max}$

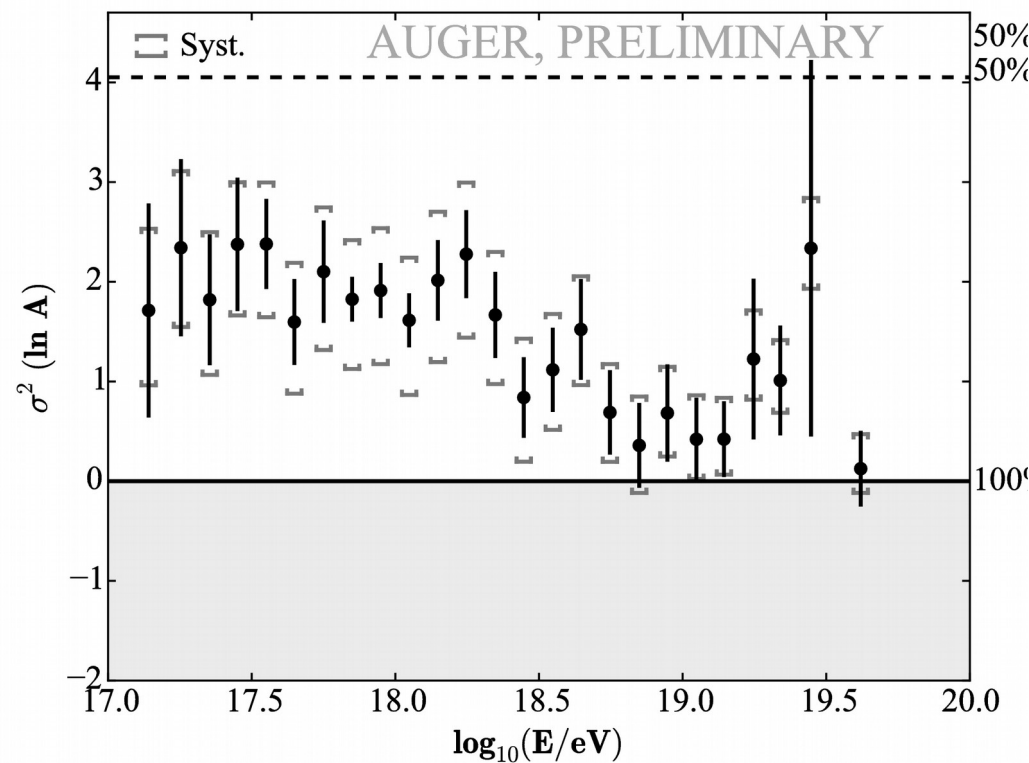


Standard FD  $\rightarrow$  PHYSICAL REVIEW D **90**, 122005 (2014)

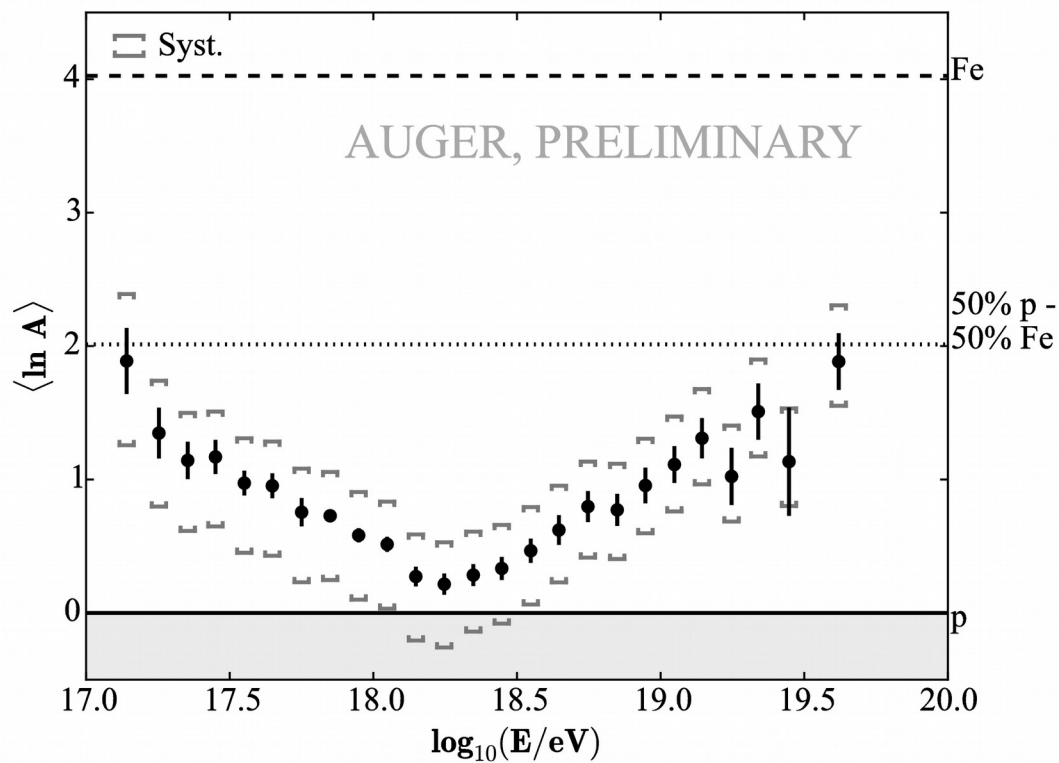
EPOS-LHC (Mean of  $\ln A$ )



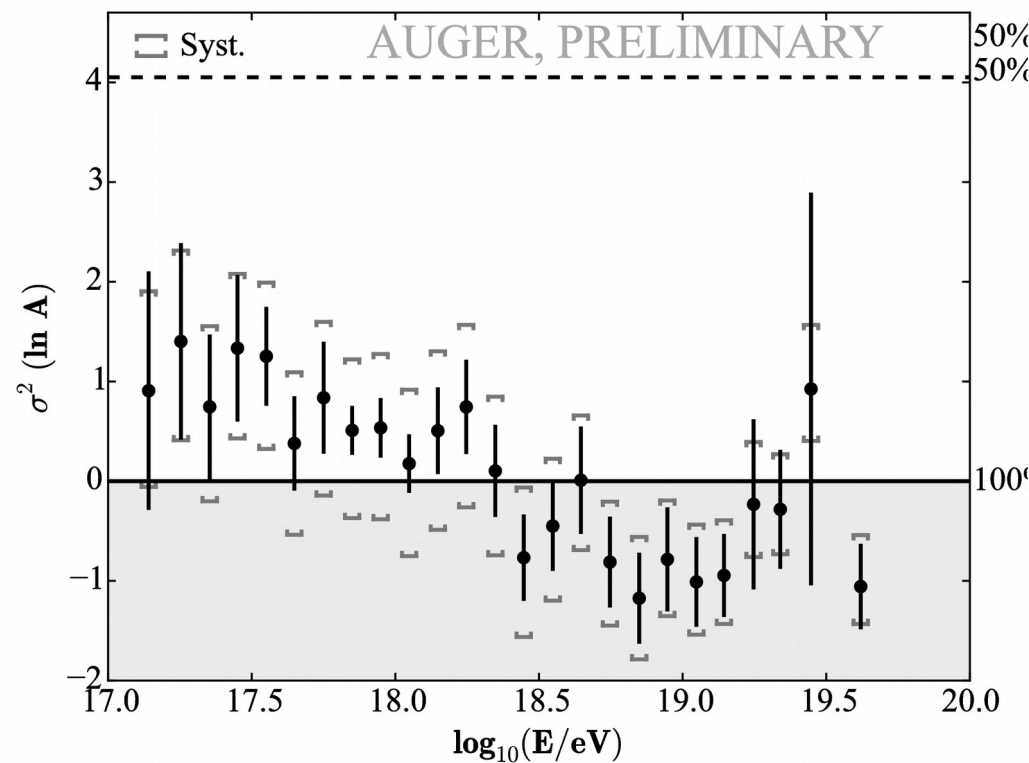
EPOS-LHC (Variance of  $\ln A$ )



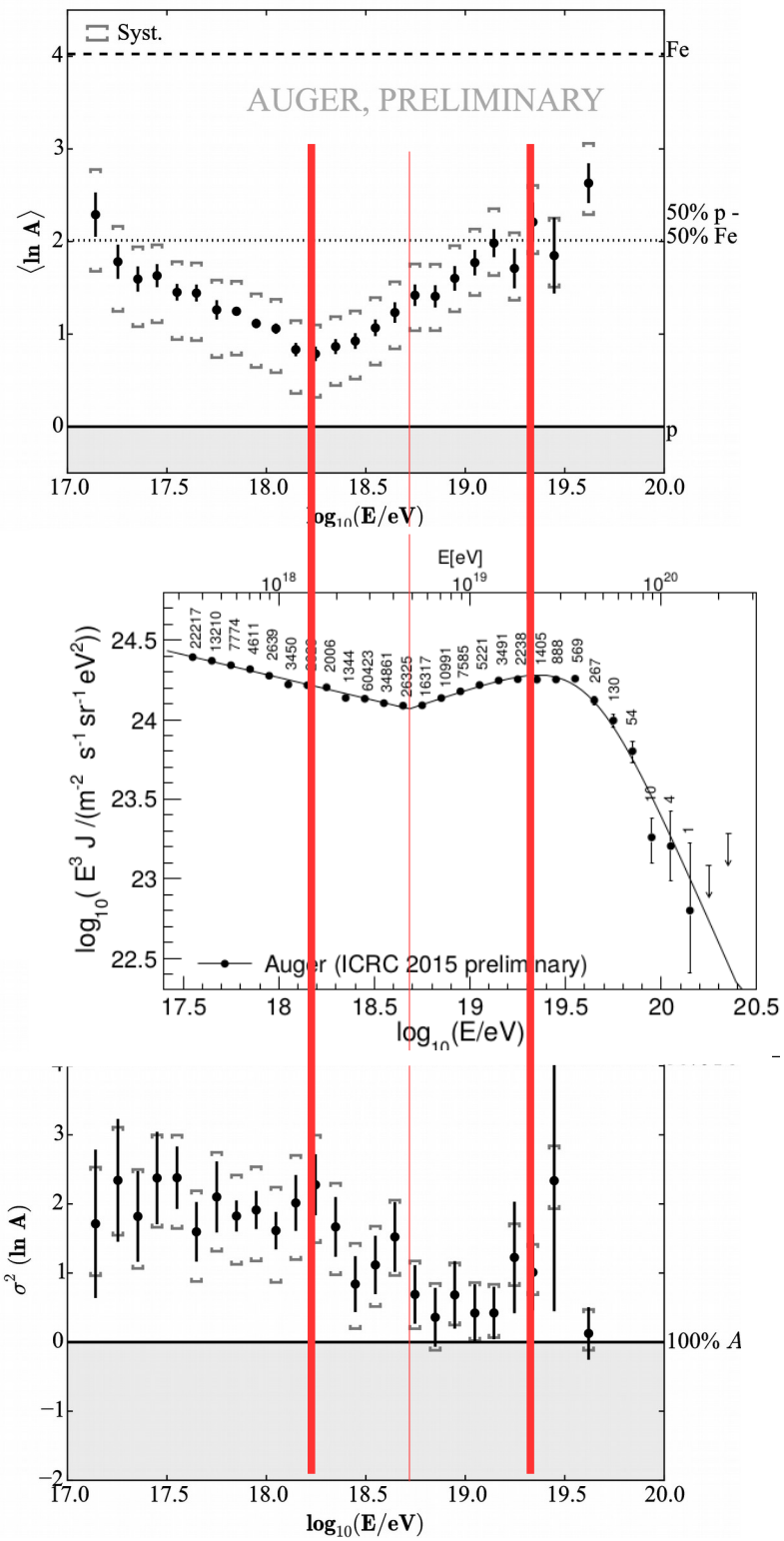
QGSJetII-04 (Mean of  $\ln A$ )



QGSJetII-04 (Variance of  $\ln A$ )



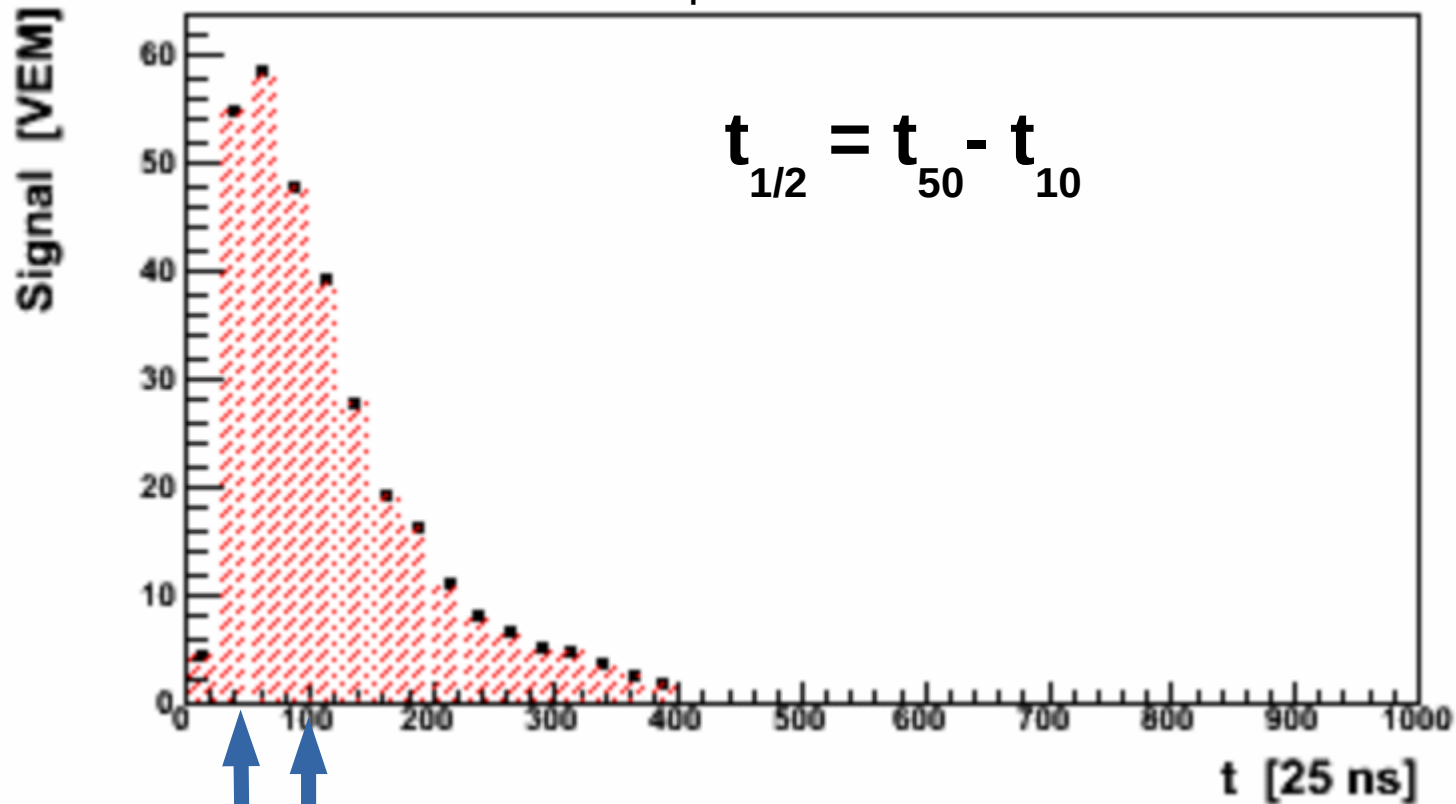
# EPOS-LHC (Mean of $\ln A$ )



# SD Observables

## Definition of rise time, ' $t_{1/2}$ '

Example of a SD trace



$t_{50}$  = time that takes to accumulate 50% of the total signal  
 $t_{10}$  = time that takes to accumulate 10% of the total signal

# Sec( $\theta_{\max}$ )

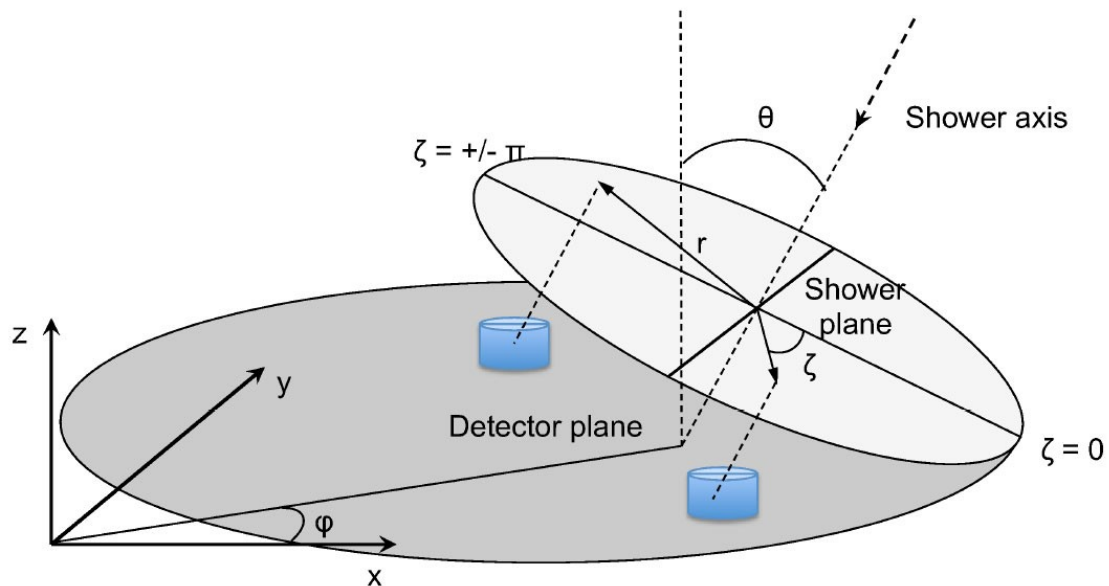
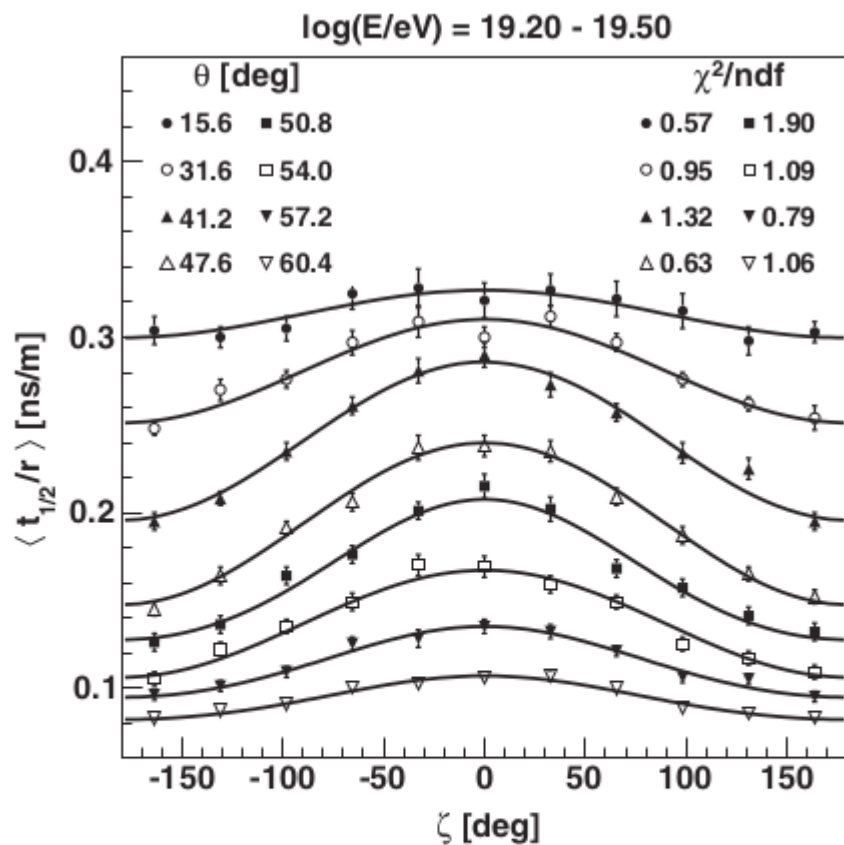
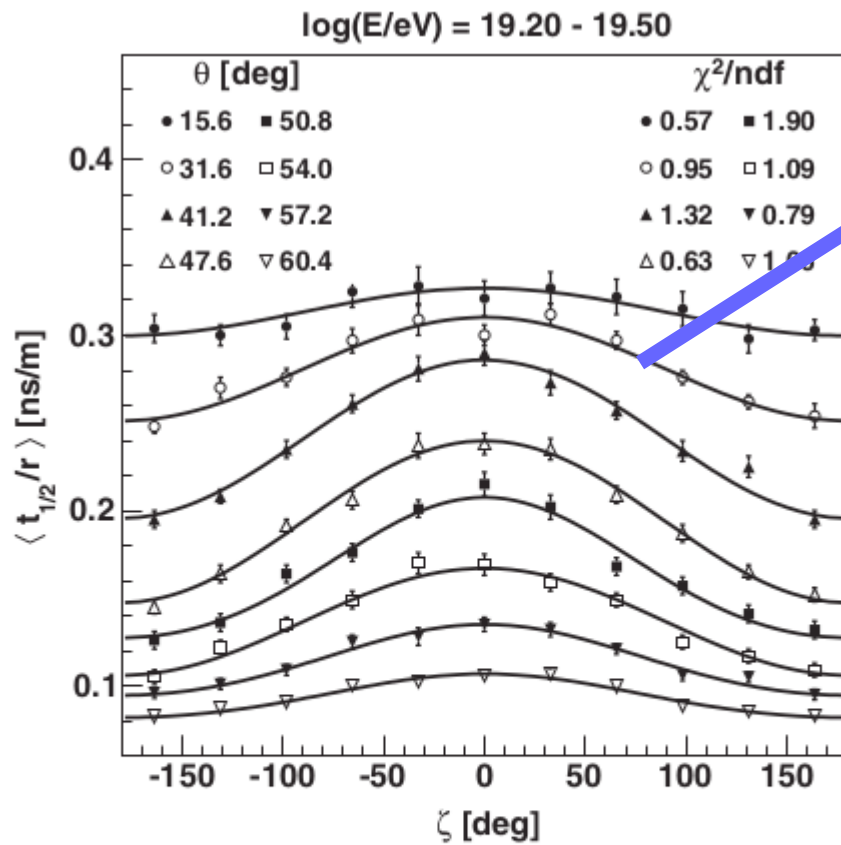


FIG. 4. Dependence of  $\langle t_{1/2}/r \rangle$  on the polar angle  $\zeta$  in the shower plane for primary energy  $\log(E/eV) = 18.55-18.70$  (top) and  $19.20-19.50$  (bottom) at different zenith angles bands. Each data point represents an average (with the corresponding uncertainty) over all stations surviving the selection criteria (see text).

# Sec( $\theta_{\max}$ )



$10^{19}$  eV (bottom panel). For each zenith-angle band the data are fitted to the function  $\langle t_{1/2}/r \rangle = a + b \cos \zeta + c \cos^2 \zeta$ . The asymmetry with respect to  $\zeta$  is evident and the ratio  $b/(a + c)$ , the so-called asymmetry factor, is used to give a measure of the asymmetry. In Fig. 4 results for a

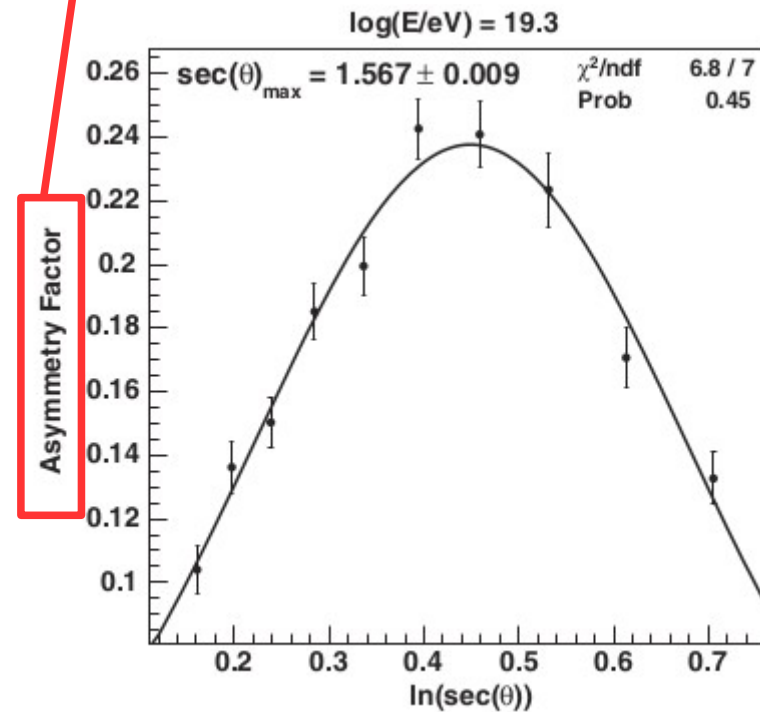


FIG. 4. Dependence of  $\langle t_{1/2}/r \rangle$  on the polar angle  $\zeta$  in the shower plane for primary energy  $\log(E/eV) = 18.55-18.70$  (top) and  $19.20-19.50$  (bottom) at different zenith angles bands. Each data point represents an average (with the corresponding uncertainty) over all stations surviving the selection criteria (see text).



$\text{Sec}(\theta_{\text{max}})$

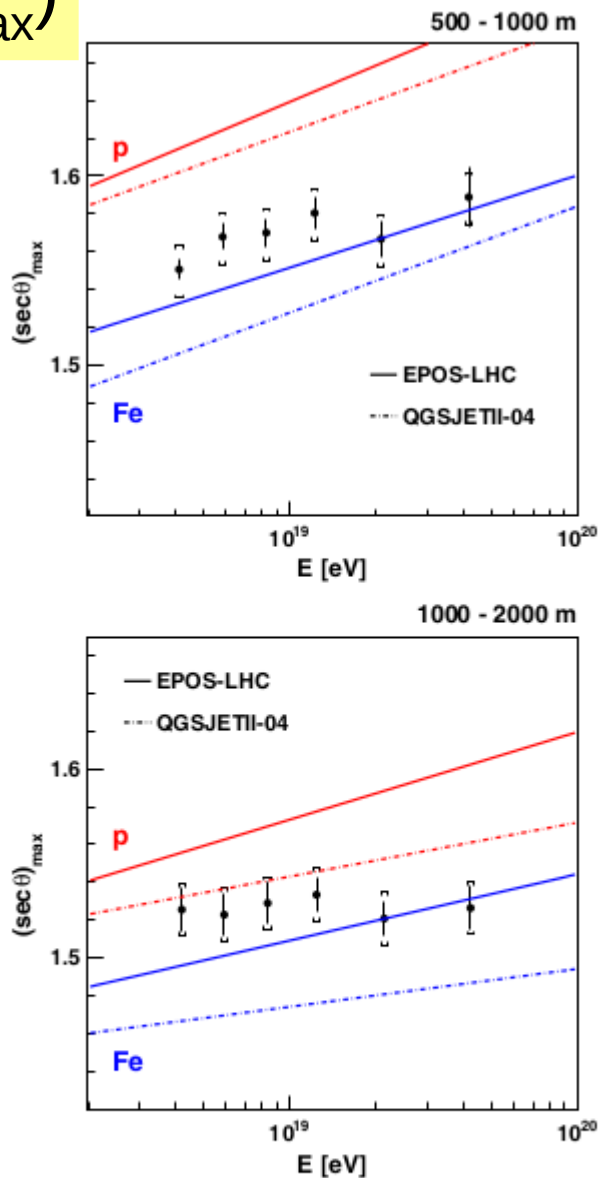


FIG. 9. Comparison between  $(\text{sec } \theta)_{\text{max}}$ , for both data and Monte Carlo predictions in the 500–1000 m interval (top) and in the 1000–2000 m interval (bottom) using both hadronic models EPOS-LHC (solid lines) and QGSJETII-04 (dashed lines), for both primaries, proton (red) and iron (blue).

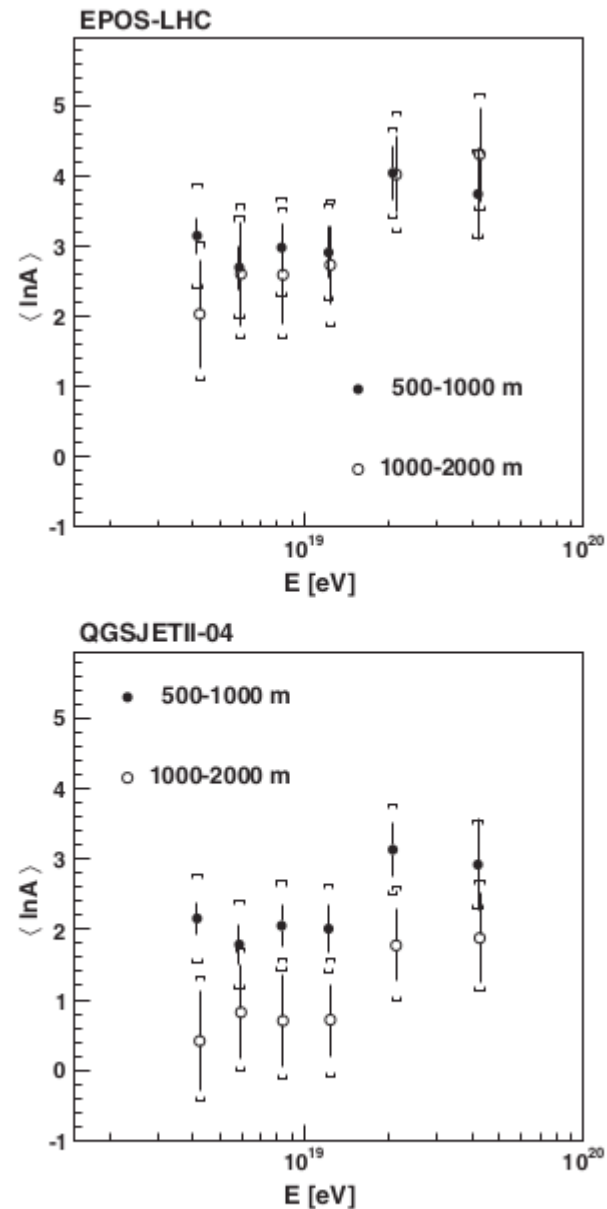


FIG. 10. Comparison of  $\langle \ln A \rangle$  as a function of energy for both core distance intervals predicted by EPOS-LHC (top panel) and QGSJETII-04 (bottom panel).

# Sec( $\theta_{\max}$ )

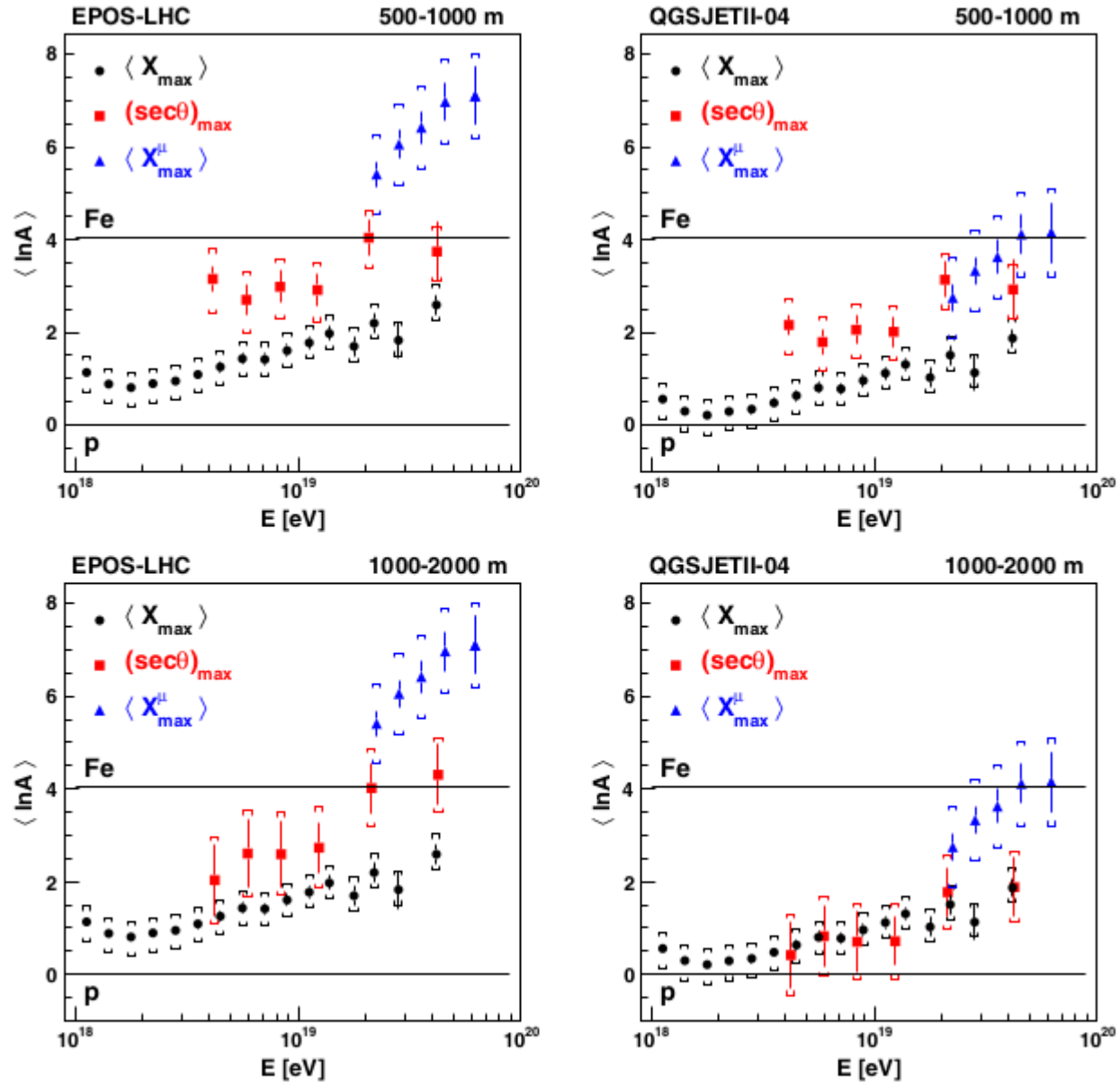
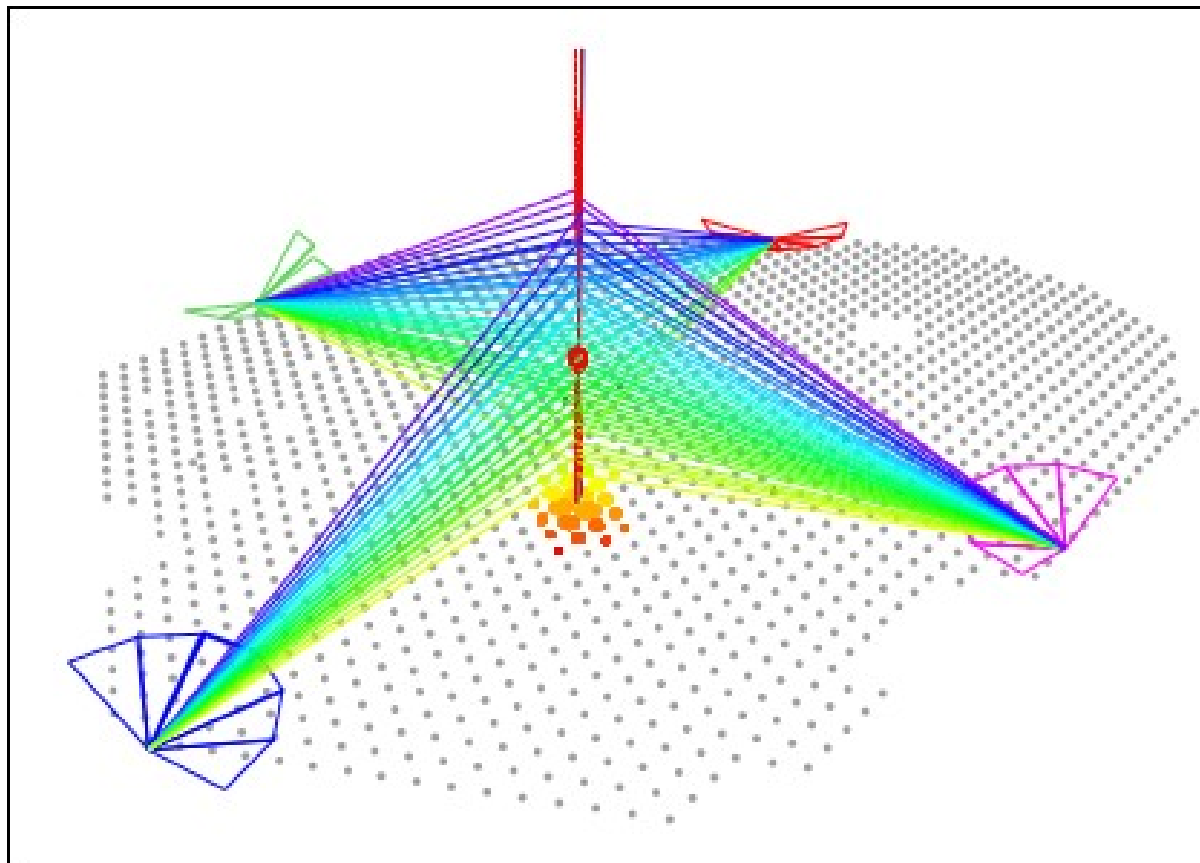


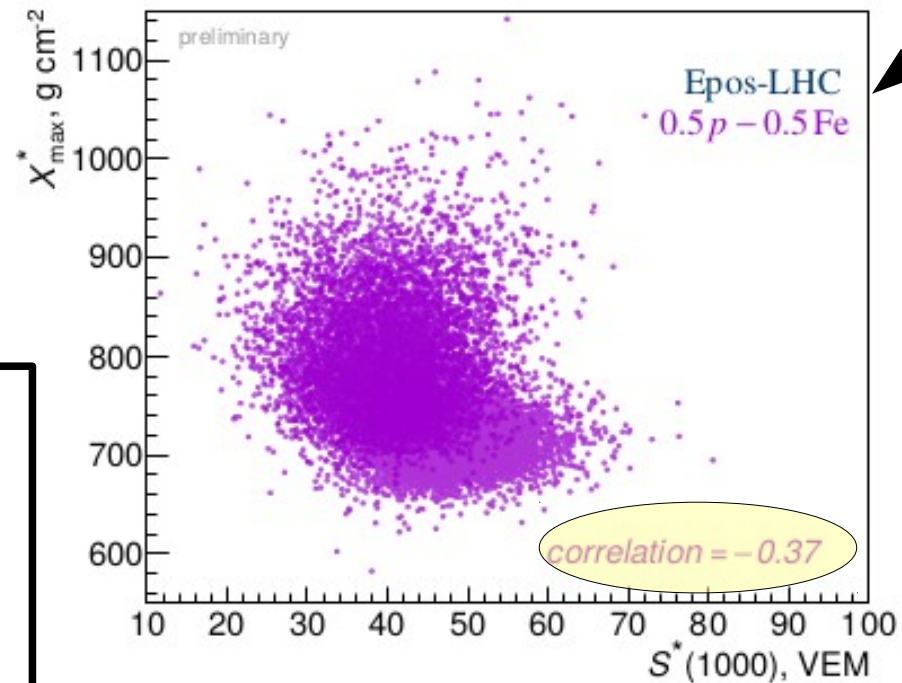
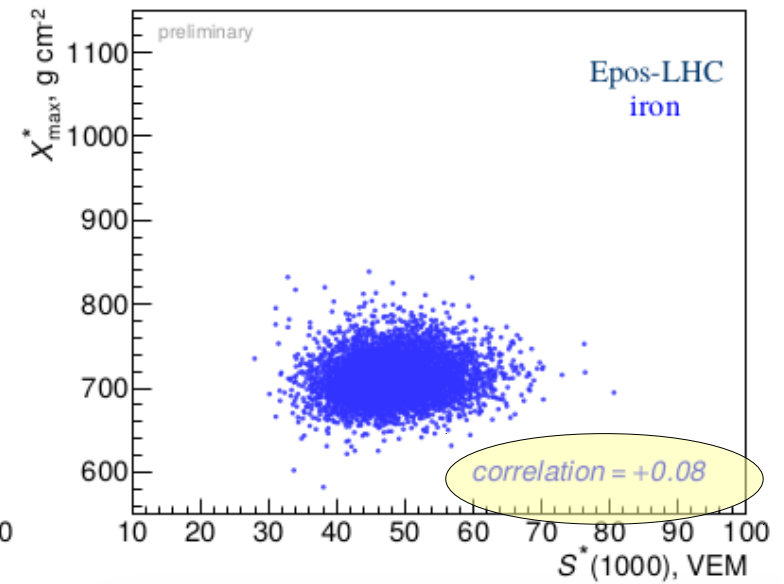
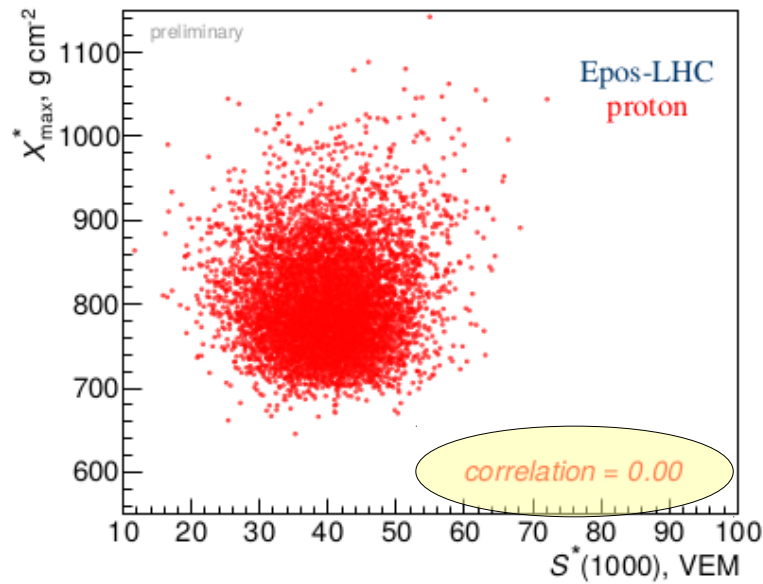
FIG. 11.  $\langle \ln A \rangle$  as a function of energy as predicted by EPOS-LHC and QGSJETII-04. Results from the asymmetry analysis in both  $r$  intervals are shown and compared with those from the elongation curve [5] and the MPD method [13].

## SD + FD Observables (hybrid events)



# Correlation factor between:

$X_{\max}^*$  and  $S_{1000}^*$

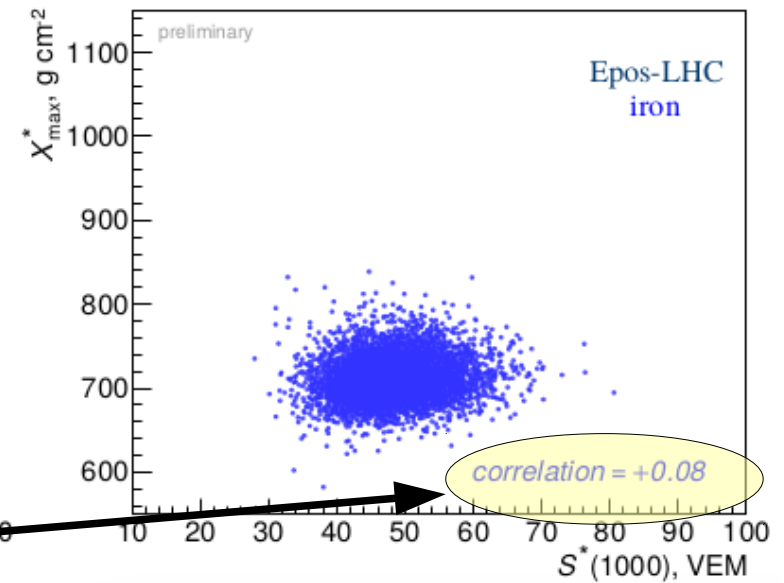
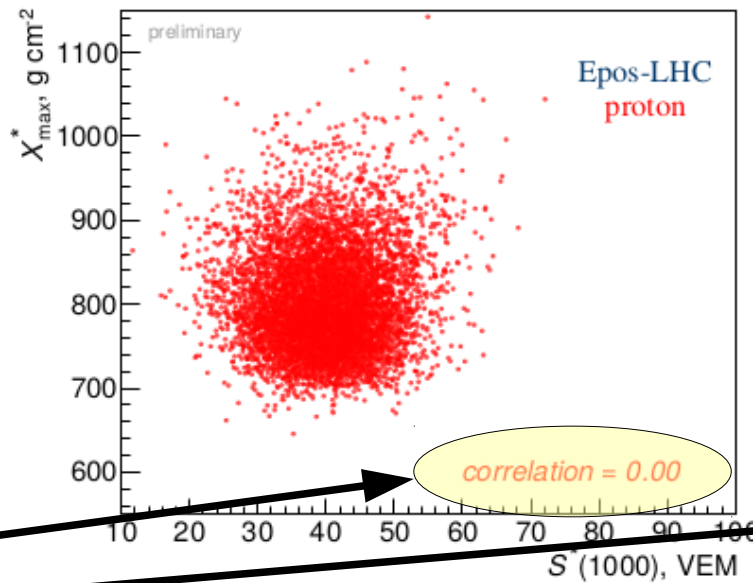


FD: depth of shower maximum,  $X_{\max}$ , scaled to 10 EeV  
SD: signal at 1000 m from the core,  $S_{(1000)}$ , scaled to 10 EeV and 38°.

The scaled observables are used, they are marked with an asterisk

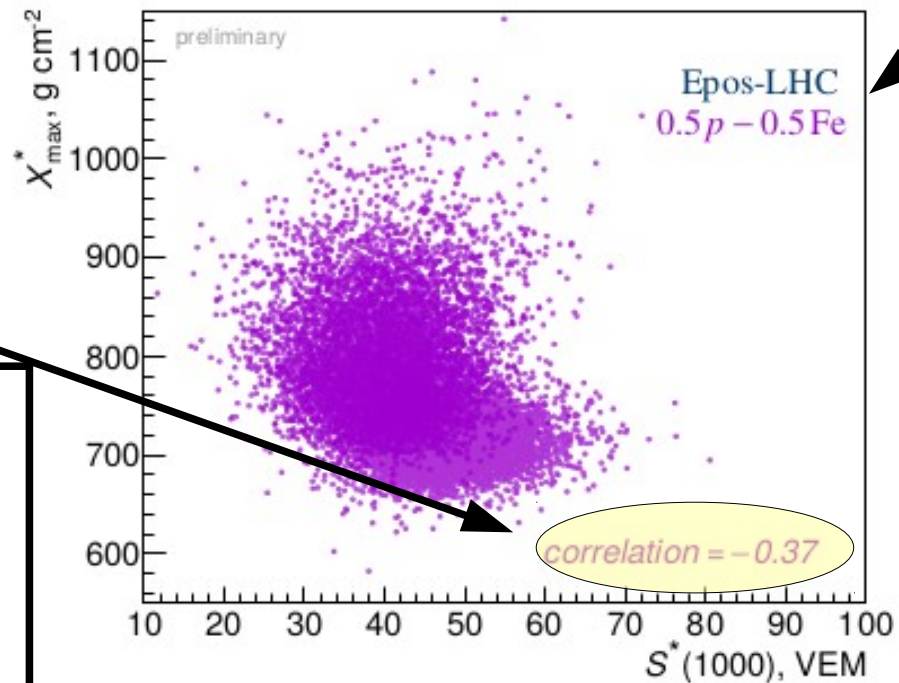
# Correlation factor between:

$X_{\max}^*$  and  $S_{1000}^*$



For pure compositions  
Correlation factor  $\approx 0$

For mixed compositions  
Correlation factor  $\neq 0$



FD: depth of shower maximum,  $X_{\max}$ , scaled to 10 EeV  
SD: signal at 1000 m from the core,  $S_{(1000)}$ , scaled to 10 EeV and  $38^\circ$ .

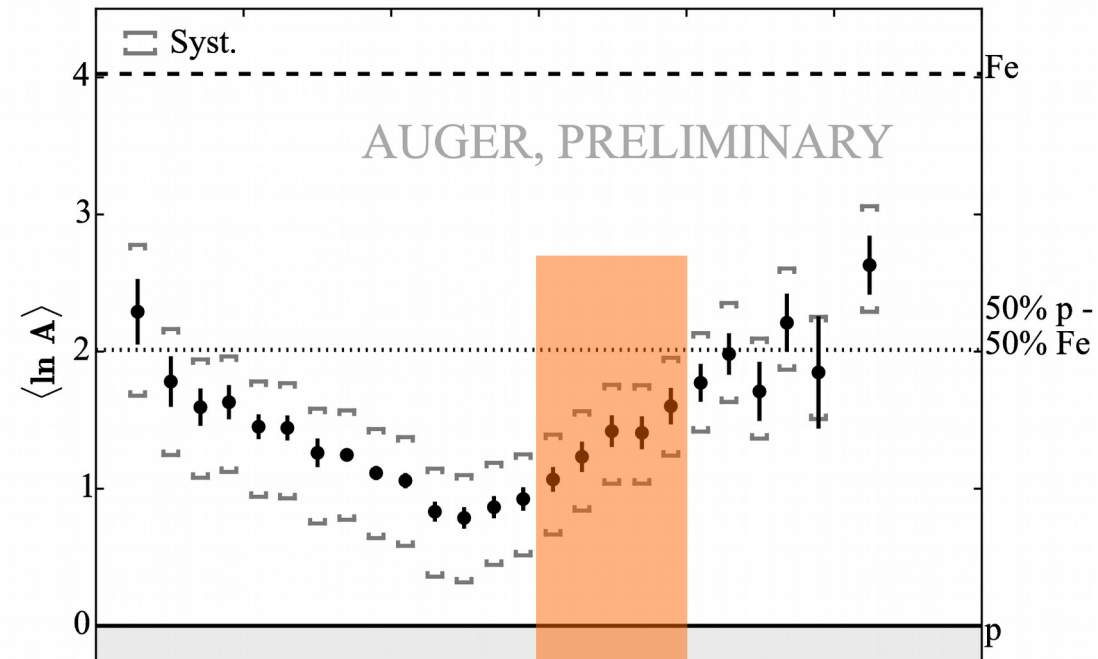
The scaled observables are used, they are marked with an asterisk

# Data

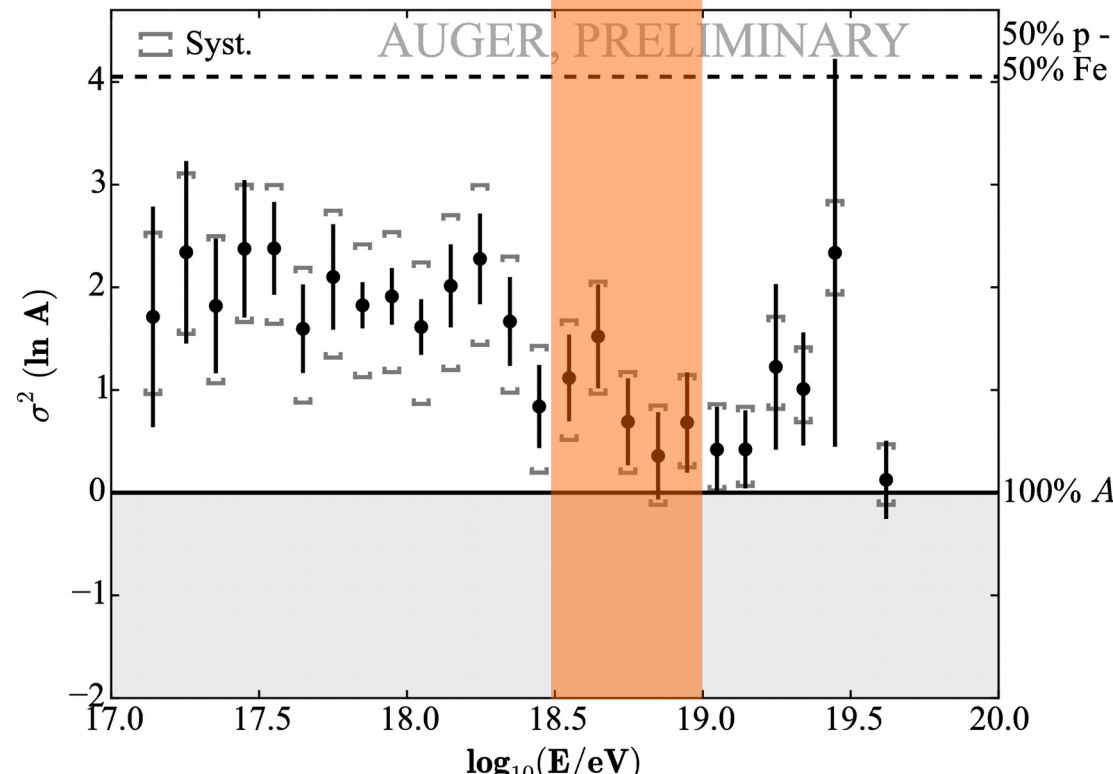
Hybrid (FD and SD)

- 8 years 12/2004 – 12/2012
- $\lg(E/eV) = 18.5 - 19.0$
- zenith angles  $0^\circ - 65^\circ$
- 1376 high-quality events

### EPOS-LHC (Mean of $\ln A$ )



### EPOS-LHC (Variance of $\ln A$ )

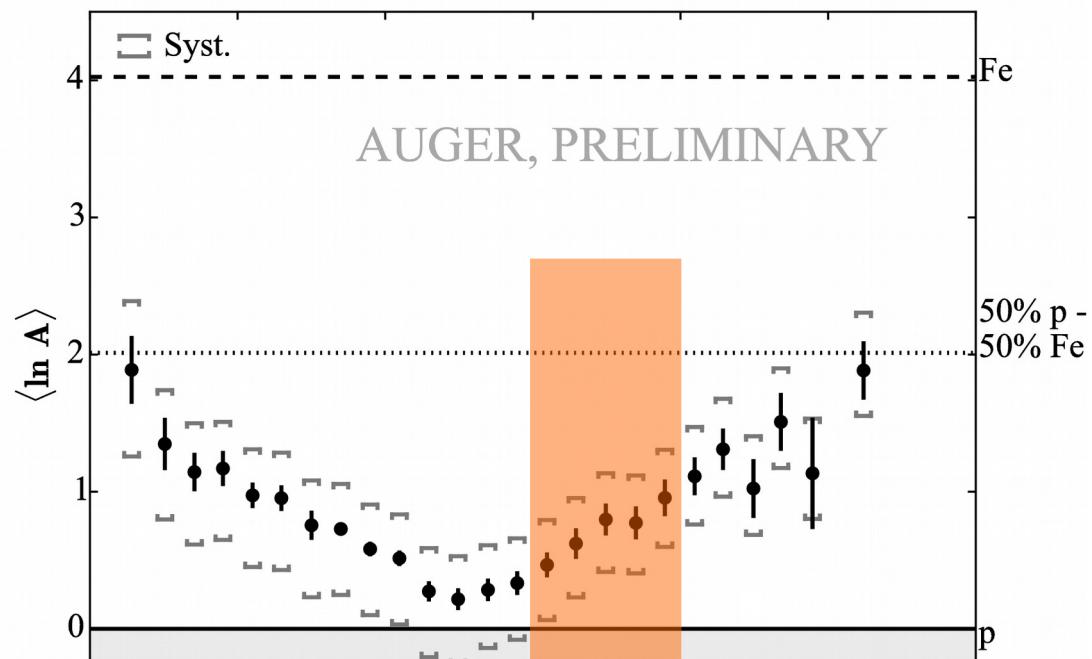


## Data

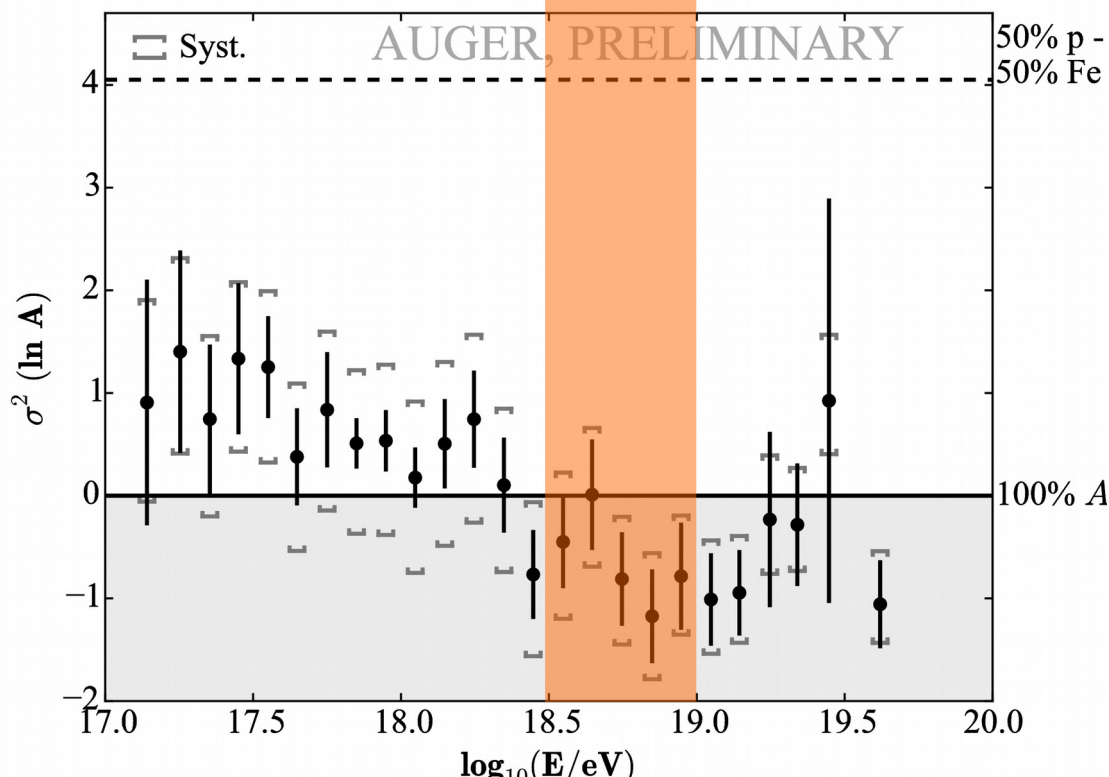
Hybrid (FD and SD)

- 8 years 12/2004 – 12/2012
- $\lg(E/eV) = 18.5 - 19.0$
- zenith angles  $0^\circ - 65^\circ$
- 1376 high-quality events

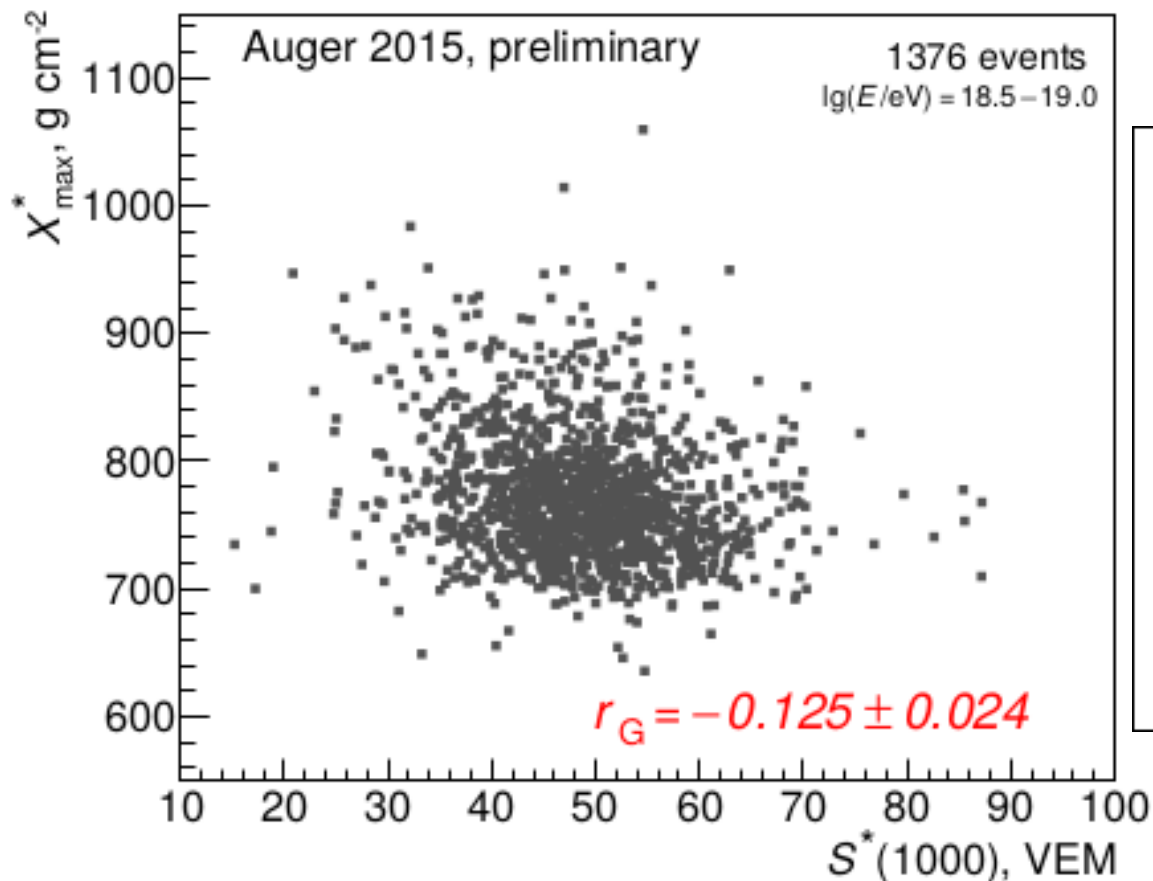
QGSJetII-04 (Mean of  $\ln A$ )



QGSJetII-04 (Variance of  $\ln A$ )



correlation is significantly negative

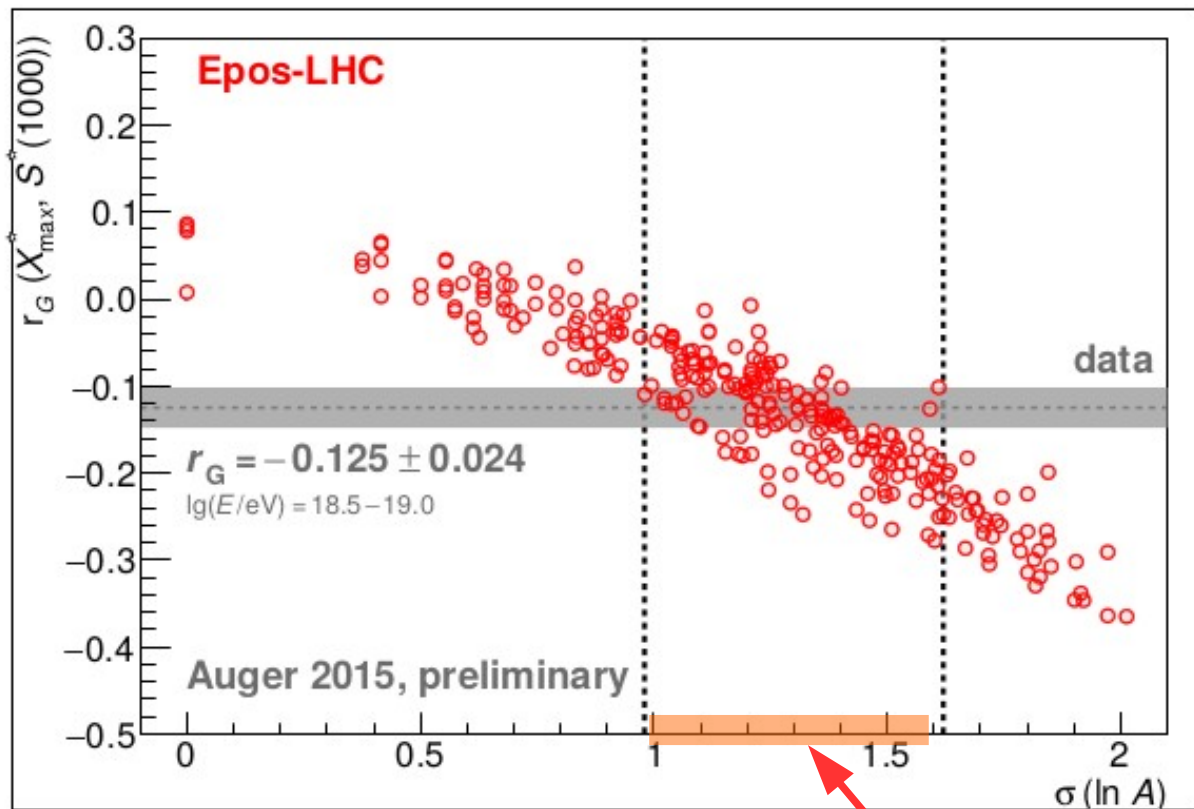


$r_G(X_{\max}^*, S^*(1000))$ for protons		
Epos-LHC	QGSJetII-04	Sibyll 2.1
0.00	+0.08	+0.07
difference to data		
$\approx 5\sigma$	$\approx 8\sigma$	$\approx 7.5\sigma$
difference is larger for other pure beams		

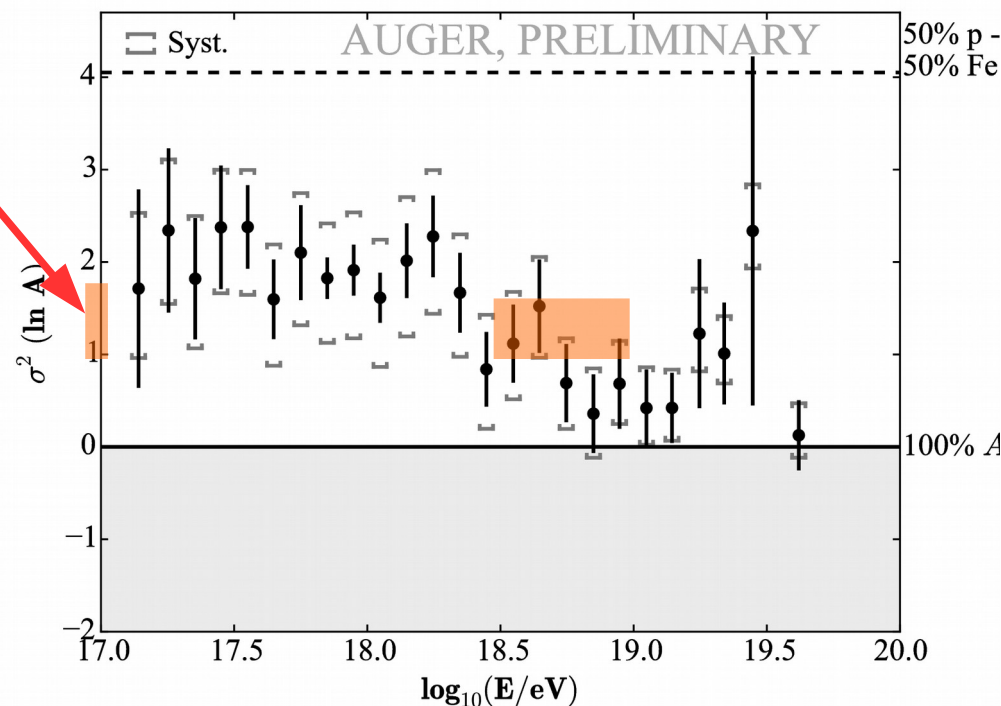
systematics plays only a minor role  $\sigma_{\text{syst}}(r_G) \lesssim 0.01$   
due to invariance of  $r_G$  to additive and multiplicative scale transformations

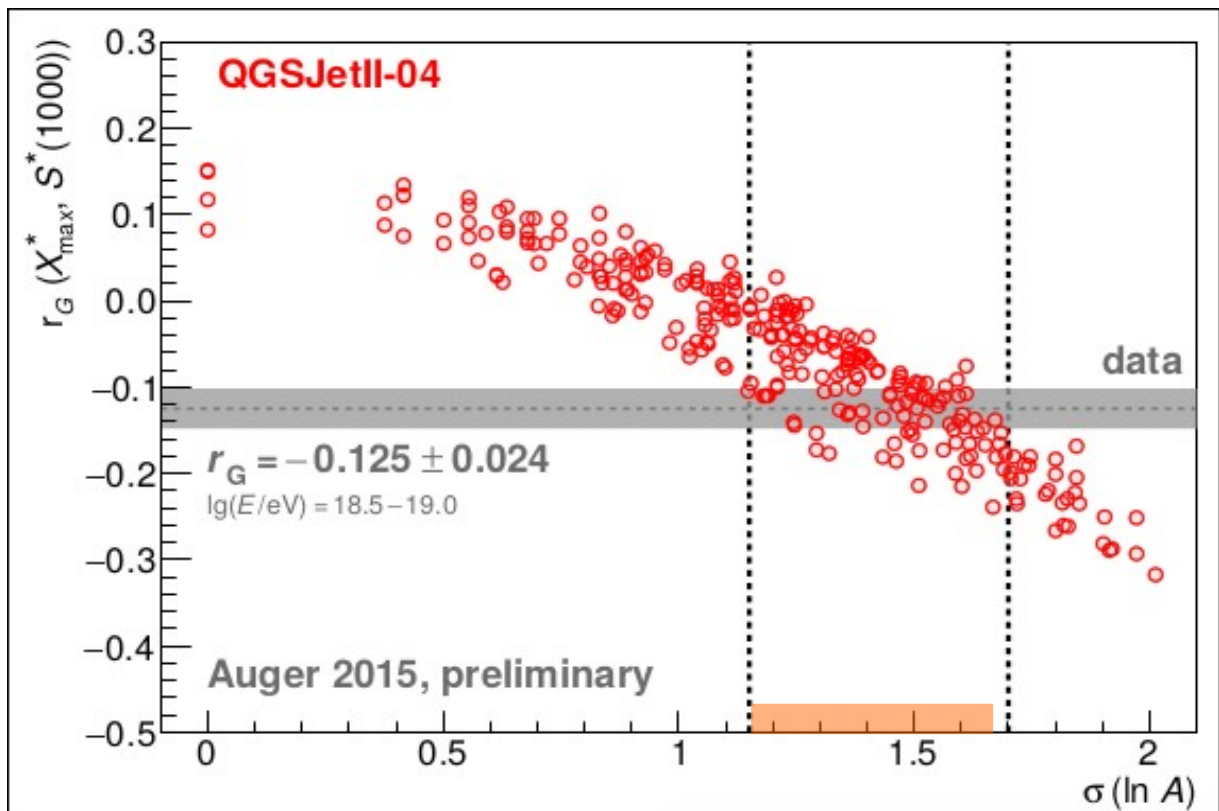
↑  
Data not consistent with  
pure composition



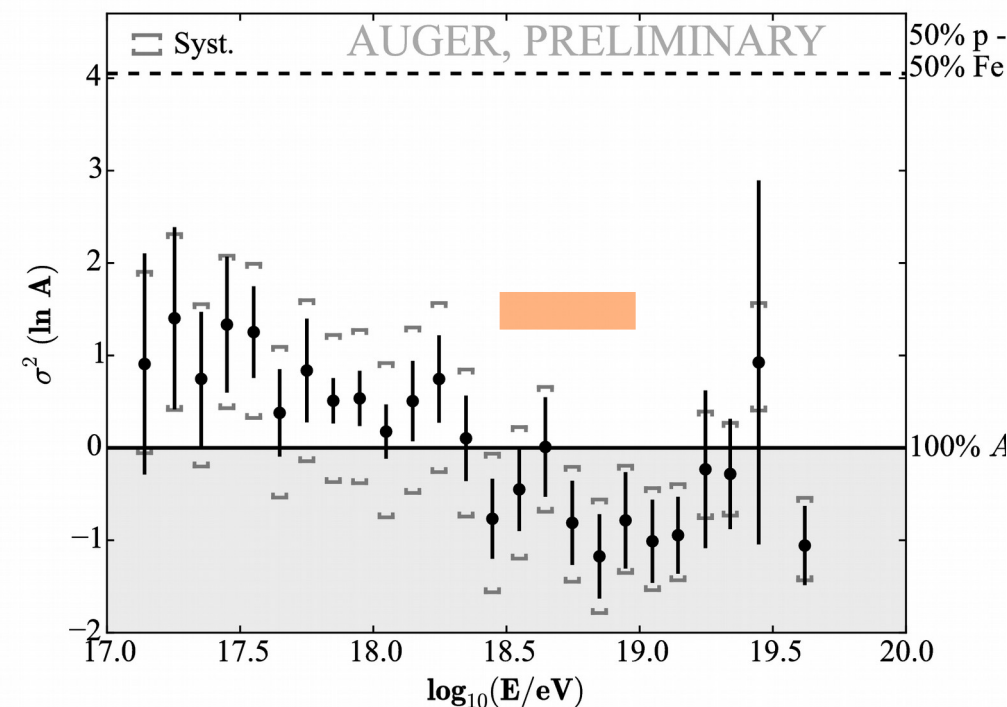


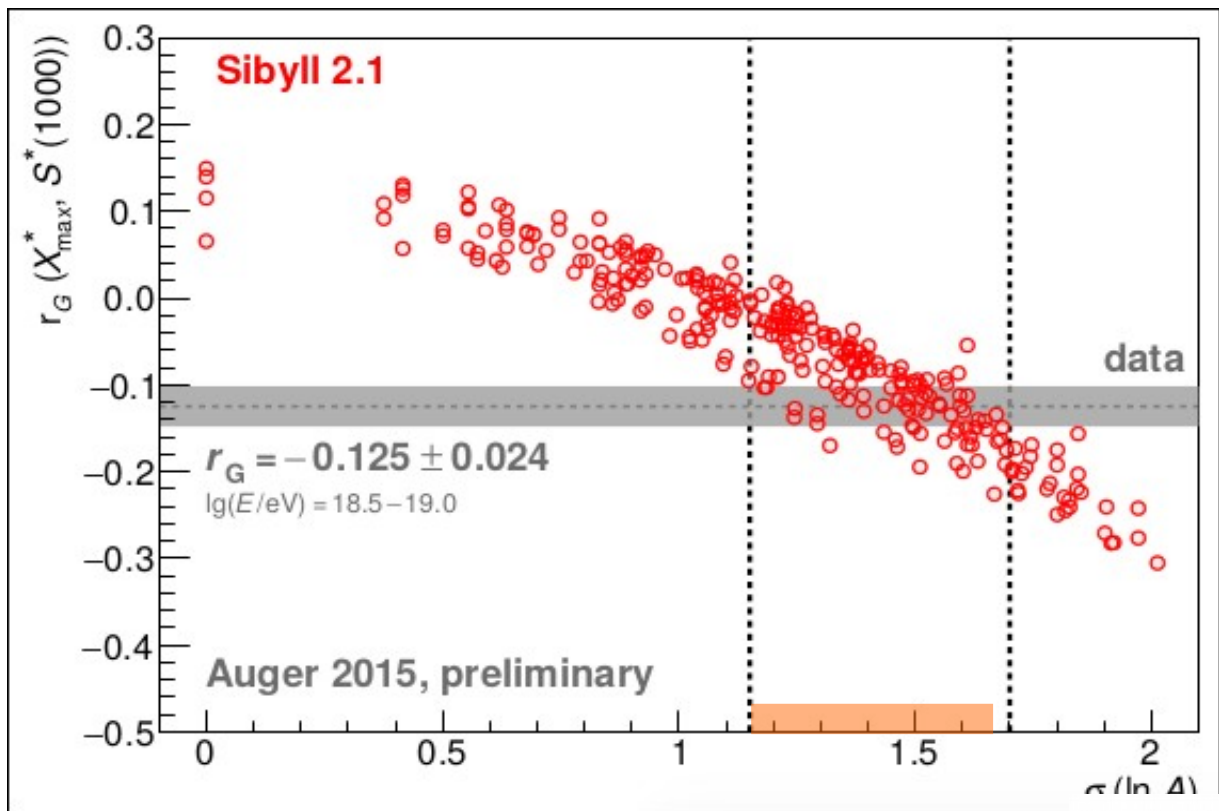
**EPOS-LHC (Variance of  $\ln A$ )**





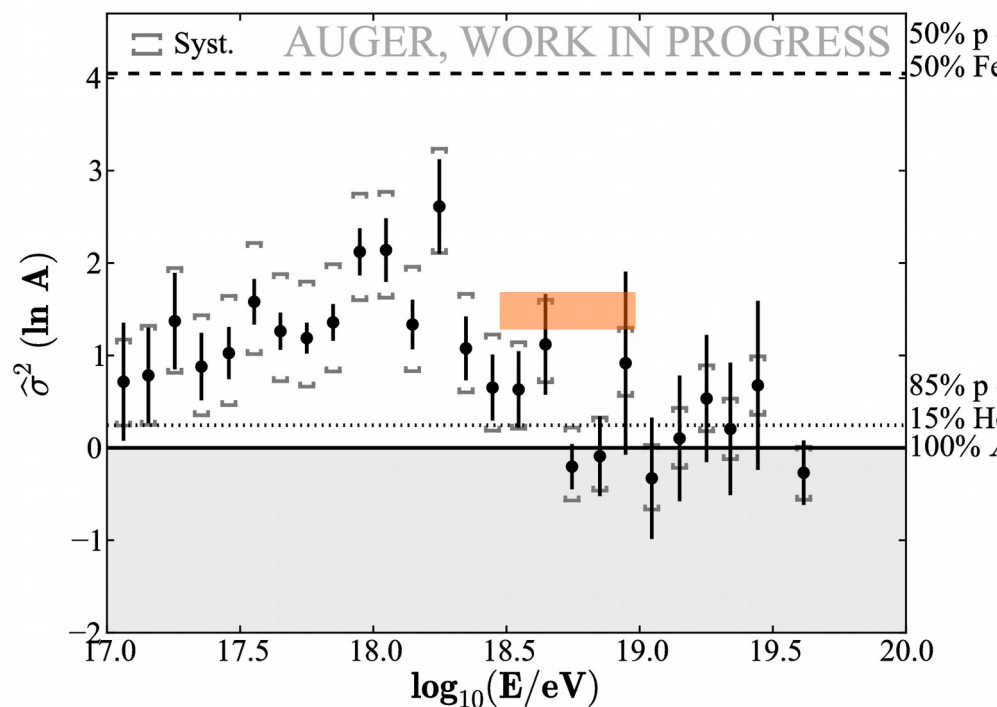
**QGSJetII-04 (Variance of ln A)**





**Sibyll2.1 (Std. Deviation of ln A)**

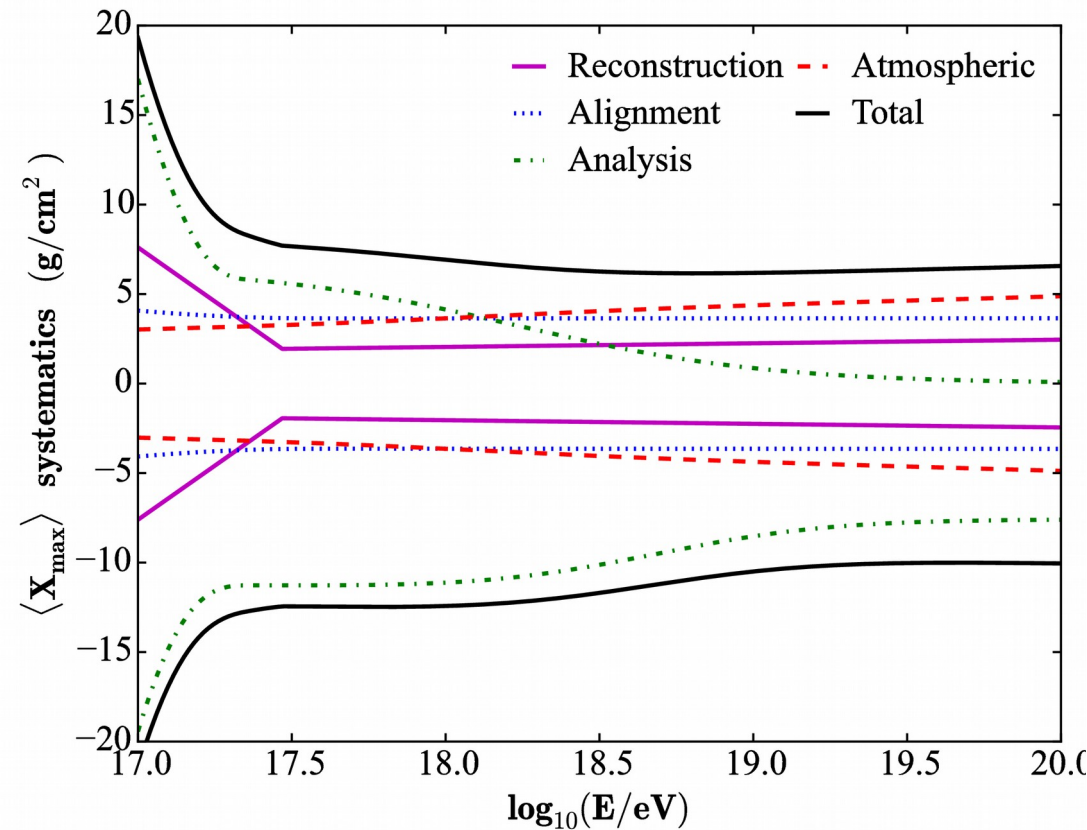
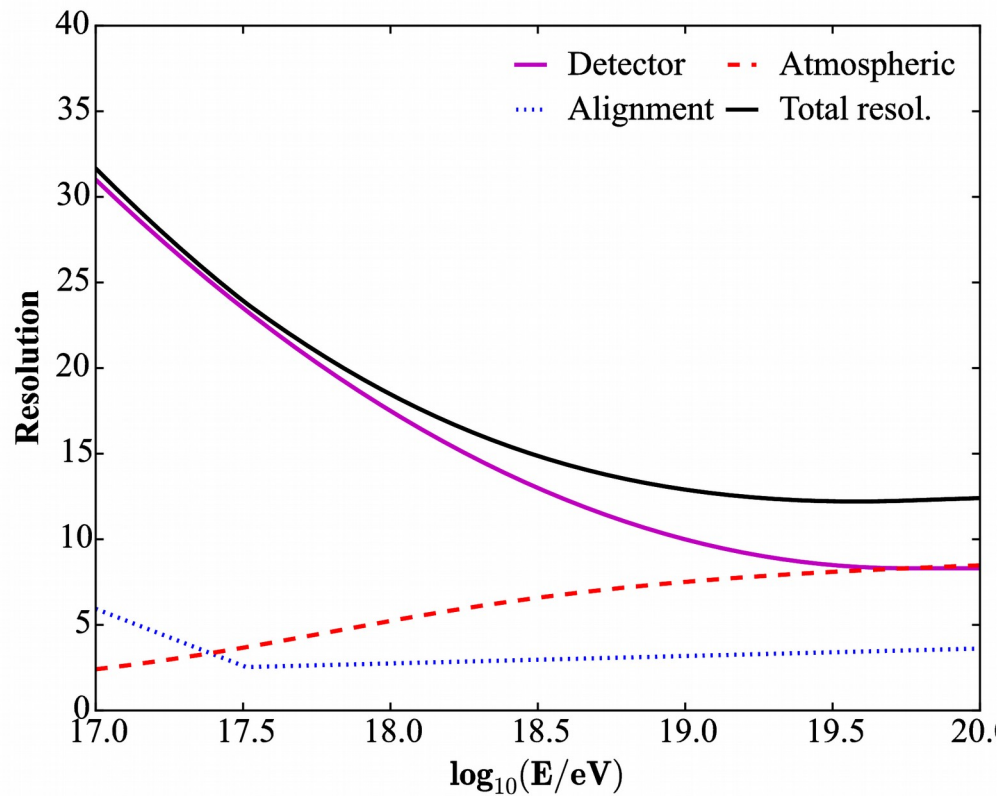
Interpretation of mass dispersion from  $S_{1000}, X_{\max}$  correlation is consistent with all models.



# Summary

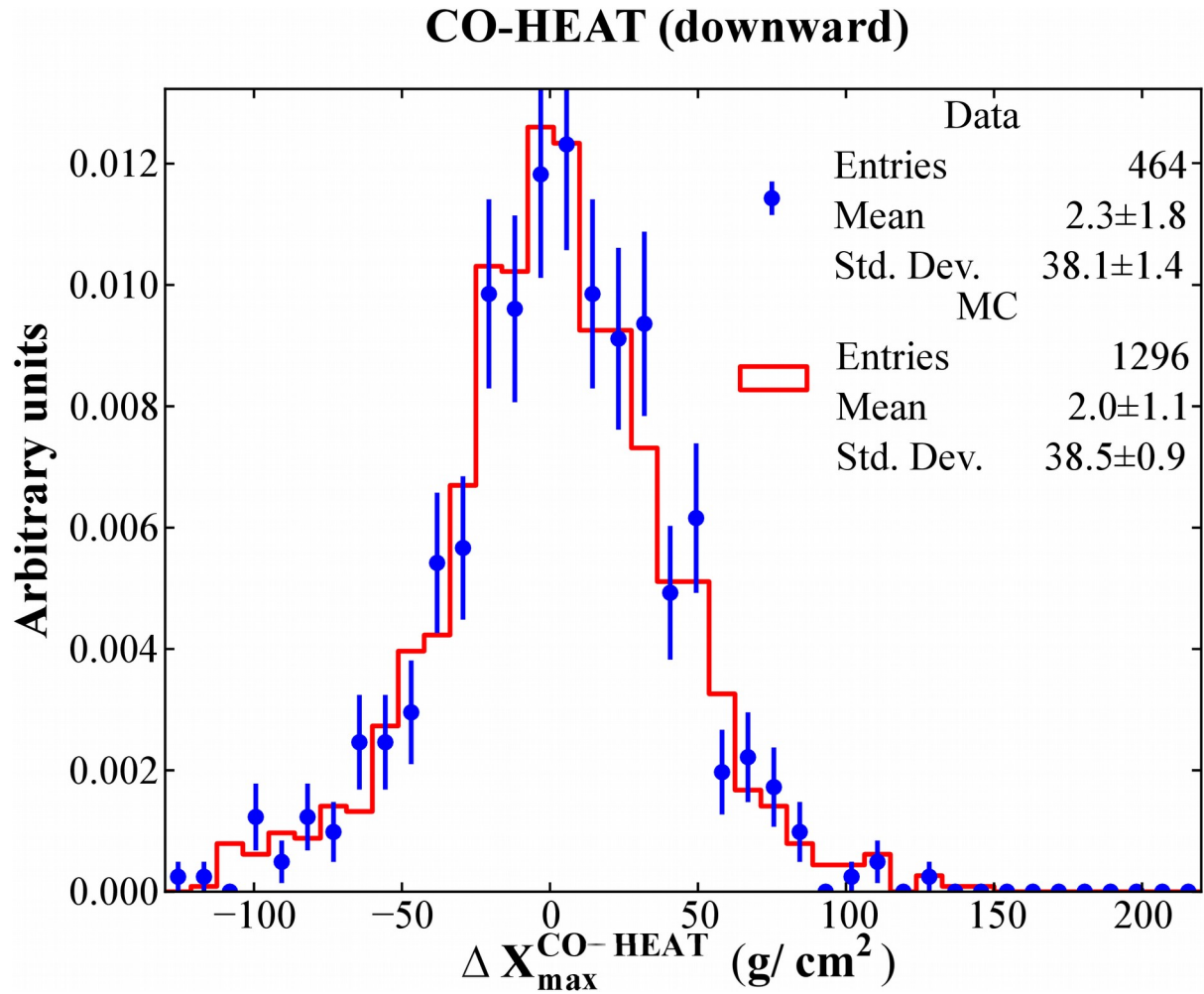
- The Pierre Auger provide a range of observables that are sensitive to different aspects (channels) of hadronic interactions in air showers.
- Observables correlated with the electromagnetic channel ( $X_{\max}$ ) provide a more reliable interpretation of the mass composition. While observables related to the muonic channel provide constraints to hadronic interaction models (details on following talk by Tanguy).
- Currently, none of the high hadronic interaction models can describe coherently all the different observables.

# Resolution and systematics of the reconstructed $X_{\max}$ for HEAT



**Note:** The detector resolution is estimated using simulations.

# Validation of the HEAT detector simulation



## Correlation between $X_{\max}^*$ and $S^*(1000)$

Ranking coefficient  $r_G$  [R. Gideon, R. Hollister, JASA 82 (1987) 656]

① rank events in  $X_{\max}^*$  and  $S^*(1000)$

② replace measured values by ranks:

$$X_{\max}^*(1), \dots, X_{\max}^*(N) \implies 1, 2, \dots, N$$

$$S^*(1000)(1), \dots, S^*(1000)(N) \implies 1, 2, \dots, N$$

③ count events with ranks deviating from the expectations for perfect (anti-)correlation; all events contribute 0 or 1  $\Rightarrow$  robustness against outliers

**$r_G$  is invariant to any transformations leaving ranks unchanged**  
e.g. to systematics in  $X_{\max}^*$  and  $S^*(1000)$

various coefficients applied (incl. Pearson, Spearman), conclusions unchanged